



## ORIGINAL ARTICLE

# Cortical Afferents of Area 10 in *Cebus* Monkeys: Implications for the Evolution of the Frontal Pole

Marcello G.P. Rosa <sup>1,2,3†</sup>, Juliana G.M. Soares<sup>4,†</sup>, Tristan A. Chaplin<sup>1,2,3</sup>, Piotr Majka<sup>1,2,3,5</sup>, Sophia Bakola<sup>1,2,3,6</sup>, Kimberley A. Phillips<sup>7,8</sup>, David H. Reser<sup>1,2,3,9</sup> and Ricardo Gattass<sup>4</sup>

<sup>1</sup>Department of Physiology, Monash University, Clayton, VIC 3800, Australia, <sup>2</sup>Neuroscience Program, Biomedicine Research Institute, Monash University, Clayton, VIC 3800, Australia, <sup>3</sup>Australian Research Council, Centre of Excellence for Integrative Brain Function, Monash University Node, Clayton, VIC 3800, Australia, <sup>4</sup>Programa de Neurobiologia, Instituto de Biofísica Carlos Chagas Filho, Universidade Federal do Rio de Janeiro, Rio de Janeiro 21941-900, Brazil, <sup>5</sup>Laboratory of Neuroinformatics, Department of Neurophysiology, Nencki Institute of Experimental Biology of Polish Academy of Sciences, 3 Pasteur Street, 02-093 Warsaw, Poland, <sup>6</sup>Department of Pharmacy and Biotechnology, University of Bologna, 40126 Bologna, Italy, <sup>7</sup>Department of Psychology, Trinity University, San Antonio, TX 78212, USA, <sup>8</sup>USA Southwest National Primate Research Center, Texas Biomedical Research Institute, San Antonio, TX, USA and <sup>9</sup>Monash Rural Health, Monash University, Churchill, VIC 3842, Australia

Address correspondence to Marcello G.P. Rosa. Email: marcello.rosa@monash.edu  [orcid.org/0000-0002-6620-6285](https://orcid.org/0000-0002-6620-6285)

<sup>†</sup>These authors contributed equally to this study, and should be considered joint first authors

## Abstract

Area 10, located in the frontal pole, is a unique specialization of the primate cortex. We studied the cortical connections of area 10 in the New World *Cebus* monkey, using injections of retrograde tracers in different parts of this area. We found that injections throughout area 10 labeled neurons in a consistent set of areas in the dorsolateral, ventrolateral, orbital, and medial parts of the frontal cortex, superior temporal association cortex, and posterior cingulate/retrosplenial region. However, sites on the midline surface of area 10 received more substantial projections from the temporal lobe, including clear auditory connections, whereas those in more lateral parts received >90% of their afferents from other frontal areas. This difference in anatomical connectivity reflects functional connectivity findings in the human brain. The pattern of connections in *Cebus* is very similar to that observed in the Old World macaque monkey, despite >40 million years of evolutionary separation, but lacks some of the connections reported in the more closely related but smaller marmoset monkey. These findings suggest that the clearer segregation observed in the human frontal pole reflects regional differences already present in early simian primates, and that overall brain mass influences the pattern of cortico-cortical connectivity.

**Key words:** connections, frontopolar cortex, New World monkey, prefrontal cortex, superior temporal cortex

The frontopolar cortex (area 10) is a part of the brain which is unique to primates, and relatively larger in humans than in any other species (Semendeferi et al. 2001; Öngür et al. 2003). Although no clear consensus about function has emerged, different models converge in suggesting that the frontopolar cortex is involved in high-order cognition, including possible roles in integrating the outcome of multiple cognitive processes (Ramnani and Owen 2004), the transition between stimulus-oriented and stimulus-independent (self-generated) modes of attention (Burgess et al. 2007), cognitive branching (Koechlin 2011), and the redistribution of executive control resources according to changing environmental and internal demands (Mansouri et al. 2017).

To date, anatomical tracing studies of the connections of area 10 have been restricted to 2 genera of simian primates: Old World macaque monkeys (*Macaca*; Jacobson and Trojanowski 1977; Barbas et al. 1999; Cavada et al. 2000; Saleem et al. 2008; Medalla and Barbas 2014) and New World marmoset monkeys (*Callithrix*; Burman et al. 2011a, 2011b). These studies have revealed that the vast majority of the anatomical inputs to area 10 arise in other high-order association areas (i.e., areas which are not involved in early stages of sensory processing, or do not have direct participation in motor control). Results obtained in macaques and marmosets converge in their key findings, including the predominance of afferents from other frontal lobe areas, the existence of long-range projections from the superior temporal and posterior cingulate association areas, and the lack of projections from the parietal and occipital lobes. However, they also differ in detail, with the marmoset area 10 reported to receive additional connections not present in macaques (Burman et al. 2011b).

One of the main unresolved issues regarding the neuroanatomy of the frontopolar cortex in nonhuman primates is whether area 10 contains functional subdivisions. Neuroimaging studies indicate that the human frontopolar cortex encompasses medial and lateral subdivisions of area 10, which have different functional and structural connectivity (Liu et al. 2013; Bludau et al. 2014; Neubert et al. 2014; Moayed et al. 2015; Orr et al. 2015; Ray et al. 2015). In comparison, imaging studies have not found evidence of a similar segregation in the macaque (Neubert et al. 2014), suggesting that some aspects of the organization of the frontal pole may be uniquely human (Koechlin 2011). Subdivision of an area into domains characterized by different combinations of afferent connections, followed by differentiation into areas, is a likely mechanism of evolutionary change in the cortex (Padberg

et al. 2007; Krubitzer 2009). However, whether there are evolutionary precursors to subdivisions of area 10 in nonhuman primates has remained unclear. To date, electrophysiological studies have not explored the question of functional subdivisions within this area (Tsujimoto et al. 2011). Moreover, although anatomical tracer studies in the marmoset have hinted at local variations in connectivity (Burman et al. 2011a, 2011b), there has been no systematic study of potential differences between the medial and lateral parts of area 10 using quantitative techniques.

Here, we report on an investigation of the cortico-cortical connections of area 10 in the tufted capuchin (*Cebus apella*), a New World monkey which has long fascinated comparative neuroscientists due to the fact that its brain resembles that of macaques (in particular, smaller species such as *Macaca fascicularis*) in terms of sulcal pattern and the location of cytoarchitectural areas (Le Gros Clark 1959; Bortoff and Strick 1993; Rosa et al. 1993; Padberg et al. 2007; Reser et al. 2014; Mayer et al. 2016). Our study addresses 2 questions. First, is area 10 in *Cebus* connectionally uniform, or does it show regional differences, which could hint at precursors of the subdivisions found in humans? Second, does the pattern of connections in *Cebus* resemble that described for the macaque, a species with which it shares brain morphology, or does it exhibit the wider connectivity described in the more closely related (but much smaller) marmoset? The answers to these questions provide further insight regarding the anatomical evolution of the primate frontal pole.

## Materials and Methods

Three adult *Cebus apella* monkeys received injections of fluorescent tracers at multiple locations within and adjacent to area 10 (Table 1). All tracers were injected using 1- $\mu$ L syringes fitted with glass micropipettes, inserted through small cuts in the dura mater. The procedures were very similar to those employed in earlier anatomical tracing studies in the marmoset monkey (Burman et al. 2011a, 2011b, 2014a).

All surgical and experimental procedures were approved by the Animal Ethics Committee of the Centro de Ciências da Saúde of the Universidade Federal do Rio de Janeiro (CEUAIBCCF189-06/16), and conformed to the guidelines of the Brazilian Federal Arouca law governing laboratory animal use and care, as well as the Australian Code of Practice for the Care and Use of Animals for Scientific Purposes. Tracer injections and histological processing

**Table 1** Characteristics of the animals and injection sites.

| Animal ID | Sex and weight | Site number | Tracer          | Volume      | Location  | Layers included | Labeled neurons (n) <sup>a</sup> |
|-----------|----------------|-------------|-----------------|-------------|---|-----------------|----------------------------------|
| FR01      | Male, 3.3 kg   | 1           | FR <sup>b</sup> | 1.0 $\mu$ L | Area 10, rostral (medial surface)                                   | 1–5             | 1314                             |
|           |                | 4           | DY <sup>c</sup> | 0.4 $\mu$ L | Area 10, rostral (dorsal surface)                                   | 1–5             | 3362                             |
|           |                | 5           | FB <sup>d</sup> | 0.4 $\mu$ L | Area 10, rostral (polar and ventral surfaces)                       | 1–6             | 3887                             |
|           |                | 3           | FE <sup>e</sup> | 1.0 $\mu$ L | Area 10, caudal (medial surface)                                    | 1–5             | 2700                             |
| FR02      | Male, 3.0 kg   | 2           | FE              | 1.0 $\mu$ L | Area 10, rostral (medial surface)                                   | 2–4             | 4642                             |
|           |                | 6           | FB              | 0.5 $\mu$ L | Area 10, rostral (polar and ventral surfaces)                       | 1–6             | 8880                             |
|           |                | 7           | FR              | 1.0 $\mu$ L | Area 10, lateral  | 1–4             | 653                              |
|           |                | 8           | DY              | 0.5 $\mu$ L | Area 10, caudal (lateral surface, possible involvement of area 12l) | 1–5             | 12 688                           |
| FR04      | Female, 2.2 kg | 9           | DY              | 0.5 $\mu$ L | Area 12, orbital  | 2–6             | 3529                             |
|           |                | 10          | FB              | 0.5 $\mu$ L | Area 9, rostral   | 1–6             | 5304                             |

<sup>a</sup>Number of cortico-cortical projection neurons forming extrinsic connections to area 10. These represent a fraction (average 42.1%, range 25.1–54.8%) of all labeled neurons charted.

<sup>b</sup>Fluororuby (tetramethylrhodamine dextran-amine MW 10 000), 10% in dH<sub>2</sub>O.

<sup>c</sup>Diamidino yellow dihydrochloride, 2% in dH<sub>2</sub>O.

<sup>d</sup>Fast blue, 2% in dH<sub>2</sub>O.

<sup>e</sup>Fluoroemerald (fluorescein dextran-amine, MW 10 000), 10% in dH<sub>2</sub>O.

were conducted at the Instituto de Biofísica Carlos Chagas Filho, Rio de Janeiro, Brazil. Microscopic examination and all steps of data analyses were performed in the Department of Physiology, Monash University.

### Tracer Injections

The animals were premedicated with a combined intramuscular injection of atropine (0.15 mg/kg) and diazepam (0.5 mg/kg), and subsequently anesthetized with ketamine (30 mg/kg i.m.). Maintenance during the surgical procedure was achieved by intramuscular administration of a 1:5 mixture of 6% ketamine and 2% xylazine. All animals received peri-operative antibiotics (penicillin G, 300 000 IU, i.m.) and dexamethasone (0.3 mg/kg, i.m.). Postsurgical analgesia was administered through fentanyl skin patches.

A craniotomy was performed over the target regions of cortex, and the tracers were deposited in 50–100 nL increments over approximately 15 min (Fig. 1). Four fluorescent tracers were used: diamidino yellow dihydrochloride (DY, 2% in dH<sub>2</sub>O) and fast blue (FB, 2% in dH<sub>2</sub>O) were obtained from Polysciences (Warrington, PA), while fluororuby (FR, 10% in dH<sub>2</sub>O) and fluoremerald (FE, 10% in dH<sub>2</sub>O) were obtained from Molecular Probes (Eugene, OR). The micropipette tip was left in place for an additional 5–10 min following the last deposit, in order to minimize leakage of the tracer into nontarget areas. Tracer leakage along the needle track was minimized by slow withdrawal. Using these techniques, necrosis associated with the penetration of the syringes and tracer deposits was localized to the immediate neighborhood of the injection sites, and was restricted to area 10 (Burman et al. 2011a). After the final injection, the bone flap excised during the craniotomy was replaced and cemented into place. The overlying tissue was sutured and the animal was allowed to recover until it could make spontaneous and coordinated movements, after which it was returned to its home cage. Each animal was carefully monitored during the 14-day postinjection survival period, during which analgesics and antibiotics were provided.

### Histological processing

At the end of the survival period, each animal was euthanized with an overdose of sodium pentobarbital (40 mg/kg, i.v.) and transcardially perfused with saline followed by 4% paraformaldehyde in phosphate buffered saline. The brain was extracted and further postfixed for 24 hrs in 4% paraformaldehyde. The perfused brains were cryoprotected in increasing concentrations of glycerol (5–15%, in 4% paraformaldehyde), then sectioned using a cryostat, at 50 μm thickness. Every 10th section was mounted unstained for fluorescence microscopy. These sections were dried and coverslipped with di-n-butyl phthalate xylene (DPX) following quick dehydration (2 × 100% ethanol) and immersion in xylene. Adjacent series of sections were stained for Nissl substance, myelin (Gallyas 1979), and cytochrome oxidase (Wong-Riley 1979).

### Definition of Cytoarchitectural Areas

Identification of areas of the *Cebus* monkey prefrontal cortex followed the cytoarchitectural criteria established by Cruz-Rizzolo et al. (2011), with the exception that we recognized area 8b as distinct from area 9, using the criteria proposed by Petrides and Pandya (1999) for the macaque.

The nomenclature of areas in the temporal lobe followed that summarized in Petrides and Pandya (2007), which we found applied well to the superior temporal gyrus and sulcus of *Cebus* (see also Colombo et al. 1996). Figure 2 illustrates the most important distinctions for interpretation of the present data. The auditory core and belt areas were prominent in Nissl-stained sections, due to the thick layer 4, and sharply defined layer 6 (Fig. 2 top, middle). Although both the thickness of layer 4 and the degree of definition of layer 6 were more prominent in the core areas than in the lateral and medial belt (MB) areas, these key characteristics could be used to distinguish these auditory areas as a group from the laterally adjacent parabelt, in which the upper and lower limits of layer 4 were less sharply defined, both caudally and rostrally (Fig. 2 top and middle, respectively).

Laterally, in the lower part of the superior temporal gyrus, cytoarchitectural area TS was poorly laminated in comparison with adjacent areas in low power views of Nissl-stained sections, in particular with respect to the degree of definition and thickness of layer 4. In macaques, the parabelt cortex is regarded as a complex of high-order unimodal auditory areas (Kajikawa et al. 2015). In contrast, the TS cortex, which is also likely to contain rostrocaudal subdivisions (Galaburda and Pandya 1983), has been shown to have polysensory properties (Baylis et al. 1987), despite a putative role in auditory cognition (Munoz-Lopez et al. 2010).

Further laterally, in the lip and upper bank of the superior temporal sulcus, cytoarchitectural areas TAa and TPO were characterized by a clearly demarcated layer 4, and large pyramidal cells near the bottom of layer 3, which created the appearance of a second Nissl-dense band above layer 4 (Seltzer and Pandya 1978; Baylis et al. 1987). Although these areas were quite similar in cytoarchitecture, they could be distinguished by the slightly thicker layer 4 in TAa, as well by myeloarchitecture (whereby the outer band of Baillarger was more prominent in TPO; data not shown; see Baylis et al. 1987 for similar observations in the macaque). In macaques, both areas appear to be sites of polysensory integration, with TAa containing a higher proportion of neurons that are responsive to auditory stimulation, in comparison with TPO (Baylis et al. 1987).

Finally, near the fundus of the superior temporal sulcus, the putative homologs of areas PGa and IPa were characterized by thinner cortex, with a defined but less prominent layer 4 in comparison with neighboring areas. The border between cytoarchitectural areas PGa and IPa could not be reliably identified in our material, which prompted us to group labeled neurons in the putative homologs of PGa and IPa into a single category for the purposes of data analysis. In macaques, these cytoarchitectural areas show polysensory responses, albeit with a heavy predominance of visually driven units (Baylis et al. 1987).

Although there has been no systematic cytoarchitectural study of the cingulate and retrosplenial areas in *Cebus*, we found that the criteria proposed by Kobayashi and Amaral (2000) were applicable in a straightforward manner. However, area prostriata, where robust visual responses can be obtained in other species of monkey, was recognized as being distinct from other parts of the cytoarchitectural area 30 complex based on its location within the calcarine sulcus (Morecraft et al. 2000; Palmer and Rosa 2006a; Yu et al. 2012). Similarly, we found that the cytoarchitectural subdivisions proposed by Blatt et al. (2003) for the macaque parahippocampal gyrus could be identified in *Cebus* (see Paxinos et al. 2012 for evidence in another species of New World monkey).

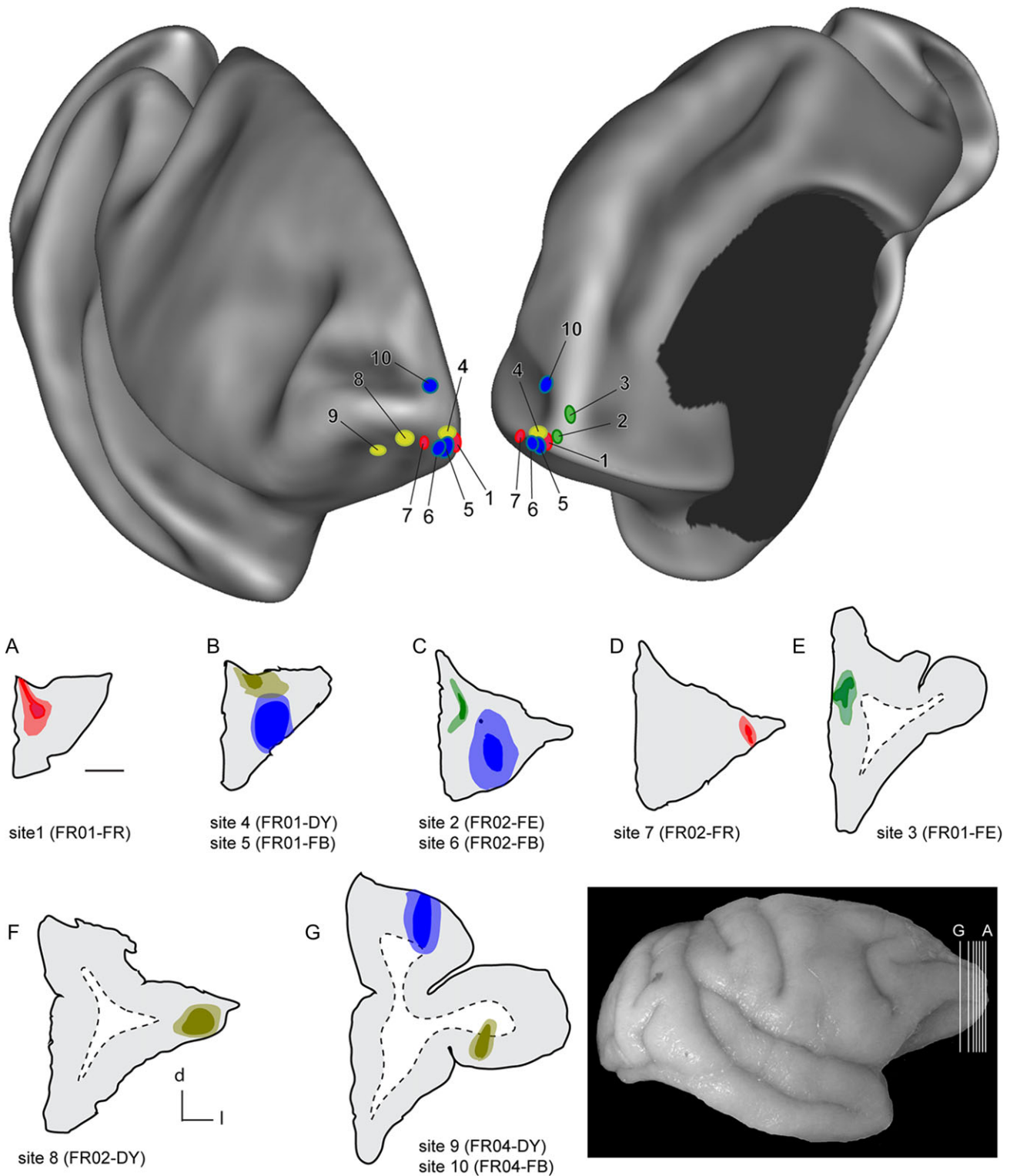


**Figure 1.** Top: Two views of a semi-inflated 3D reconstruction of the right hemisphere of a *Cebus* monkey, showing the locations of the 10 injection sites reported in this study. This reconstruction was prepared using the program CARET (Van Essen et al. 2001), based on MRI-guided alignment of midthickness cortical contours. Data from 3 animals were registered to this template. The left view is from a rostralateral perspective, and the right view from a rostromedial perspective. The color of the ovals corresponds to the tracer used (blue: FB; yellow: DY; red: FR; green: FE). Bottom: coronal sections through the centers of the injection sites in 3 animals. The gray-white matter interfaces are indicated by dashed lines. Scale bar (near section A) = 2 mm. The anatomical orientation of the sections is given by the key near panel F (d—dorsal, l—lateral). The insert (bottom right) shows the approximate level of the sections, relative to the brain of animal FR01.

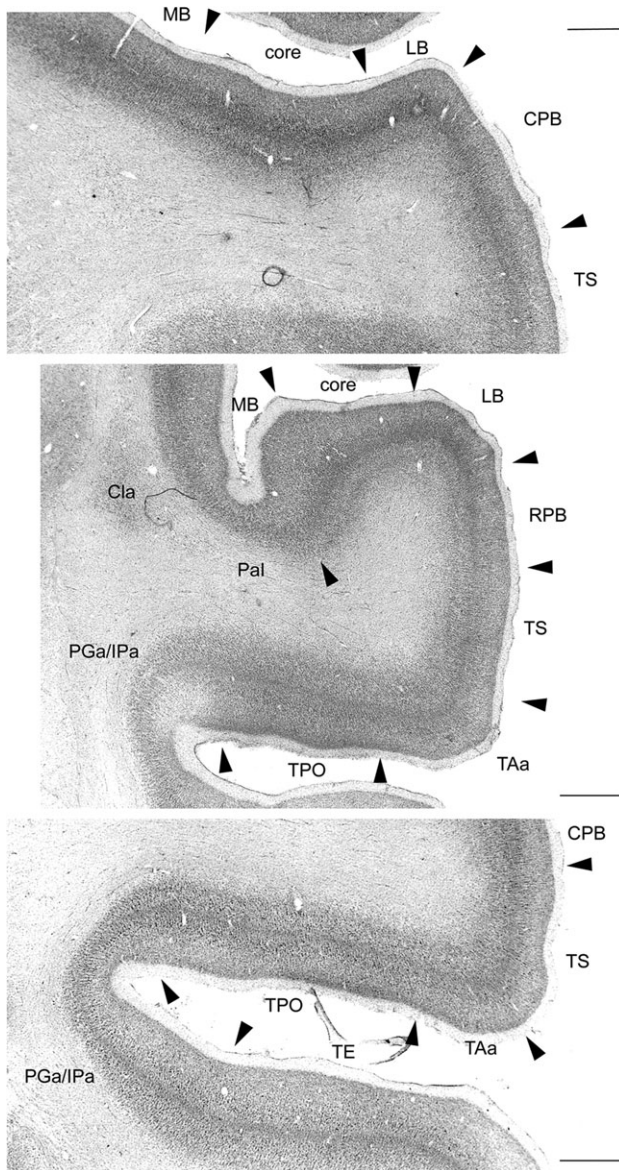


**Figure 2.** Low power photomicrographs showing the cytoarchitectural criteria used to distinguish areas in the superior temporal cortex of *Cebus*. Cytoarchitectural transitions are indicated by arrowheads. Top: Section through the lower bank of the lateral sulcus and superior temporal gyrus, at the level of the primary auditory cortex (part of the auditory core), showing transitions to the lateral belt (LB) and MB, as well as the characteristics of the caudal parabelt (CPB) and cytoarchitectural area TS. Middle: Rostral section, at the level of the rostral auditory field (indicated as “core”). The transitions between the LB and MB areas to the rostral parabelt (RPB) and parainsular (Pal) cytoarchitectural areas are indicated. TAa, TPO, and PGa/IPa are cytoarchitectural areas defined by Pandya and colleagues in the macaque (e.g., Seltzer and Pandya 1978). Cla—claustrum. Bottom: A section at a level similar to the one shown in the top panel, showing the transitions between polysensory areas in the superior temporal gyrus and sulcus. Scale bars = 1 mm.

### Data Analysis

We followed the criteria defined by Condé (1987) to estimate the dimensions of the DY and FB injection sites, and those proposed by Schmued (1990) to estimate the extent of the FE and FR injection sites (see Burman et al. 2011a for examples of injection sites using the same techniques employed in the present study). For localization of labeled neurons, the unstained sections were

examined using a Zeiss Axioplan fluorescence microscope, and labeled cell bodies were plotted with an X-Y stage digitizer (MD-3, Accustage) and associated software (MD-Plot, v. 5.3; see Burman et al. 2011b, 2015 for examples of neurons that satisfied the criteria for inclusion). The entire cortex, from the frontal to the occipital pole, was examined for fluorescent cell bodies. Digital files containing the position of each labeled neuron, together with the outlines of the injection sites, the inner and outer boundaries of the cortex, and other anatomical landmarks were imported into Adobe Illustrator, which was used to align the locations of labeled cells with images of the cortical cytoarchitecture. These images were used to quantify the numbers of labeled neurons in each cytoarchitectural area, using inbuilt functions of Adobe Illustrator. For each injection the percentages of extrinsic labeled neurons in each area were estimated as percentages of the total number of neurons, following exclusion of those cells which were found to be within the boundaries of area 10 (Table 1).

3D and 2D computer graphic reconstructions were then used to visualize the distribution of labeled neurons throughout the cortex. Alignment of sections for the 3D reconstruction was based on a template generated from an MRI scan obtained from an adult male *Cebus apella* at the Neuroscience Imaging Center, University of Pittsburgh, using a Siemens Allegra 3.0 Tesla scanner (for details, see Phillips et al. 2007). Once the histological sections were aligned, midthickness contours were manually traced, and the program CARET (Computerized Anatomical Reconstruction and Editing Toolkit, RRID:nif-0000-00279; Van Essen et al. 2001) was used to convert the resultant series of contours into a 3D triangular mesh. The coordinates describing the locations of labeled neurons were extracted from the MD-Plot data files using CARET, and projected to the nearest polygon in the mesh. Finally, the 3D surfaces were computationally flattened using standard features of CARET.

Comparison with the distribution of labeled neurons following injections in area 10 in the marmoset monkey (see Fig. 15 below) is based on data publicly available through the Marmoset Brain Architecture Project (<http://marmoset.braincircuits.org>; Majka et al. 2016).

### Results

We placed 10 injections of fluorescent tracers near the frontal pole of *Cebus* monkeys (Fig. 1). Our analyses indicate that 7 of these injections (sites 1–7) were entirely confined to area 10, according to the cytoarchitectural criteria reported by Cruz-Rizzolo et al. (2011). One injection may have straddled the caudal border of area 10 with the rostral part of area 12 lateral (12l, site 8), but revealed a pattern of connections that was highly consistent with other injections in area 10 (observation of the cytoarchitectural boundary between areas 10 and 12 was obscured by the injection site). Finally, 2 injections were located entirely caudal to area 10 (area 12 orbital [12o] in site 9; area 9 in site 10). Drawings of sections through the centers of the injection sites are illustrated in the lower part of Figure 1. Reconstruction of the injection sites across different sections (Table 1) demonstrated that sites 1–3, 5, 6, 9, and 10 included layer 4, as well as both the supragranular and infragranular layers of the frontal cortex, whereas site 2 was restricted to layers 2–4, and site 7 to layers 1–4.

Our main findings can be summarized as follows. Injections throughout area 10 labeled a similar, and very specific set of cortical areas. The vast majority of afferents originated in the dorsolateral prefrontal cortex (areas 9 and 46, and a smaller contribution from area 8b), the orbitofrontal cortex (areas 11 and 13), the lateral and orbital subdivisions of ventrolateral prefrontal area 12, and

the medial frontal cortex (areas 14 and 32). Other sources of afferents included the superior temporal auditory (TAa and TS) and polysensory (TPO, PGa, and IPa) association areas, the orbital insular and parainsular (Pal) regions, and the posterior cingulate/retrosplenial areas (23, 29, 30, and prostriata). However, as detailed below, the percentage of labeled cells in the different areas varied in a systematic manner, depending on the location of the injection site. The pattern of connections to area 10 in *Cebus* resembled, in all qualitative aspects, descriptions from previous studies in the macaque, while lacking evidence of the more widespread pattern of cortical afferents reported in the more closely related but substantially smaller marmoset monkey.

### Injections in Medial Area 10

As an initial test of the hypothesis that the New World monkey frontal pole contains subregions characterized by different sets

of afferents, we subdivided our sample into 2 groups: area 10 injections restricted to the cortex along the midline of the cerebral hemispheres (sites 1–3, from rostral to caudal), and more lateral injections (sites 4–8). This analysis (Table 2) revealed that midline injections resulted in relatively high percentages of labeled neurons outside the frontal lobe (24.1–37.8%), whereas other injections resulted in much lower percentages (5.5–10.6%). The detailed analyses described below highlight the similarities and differences between injections within these groups.

The location of labeled neurons following 2 of the midline injections is exemplified in Figure 3, which shows a series of coronal sections from animal FR01. The fluororuby injection (site 1) was located near the apex of the frontal pole, and the fluoroemerald injection (site 3) was located more caudally. Despite local variations in density, neurons labeled from these injections overlapped extensively. 2D reconstructions of the cortex and quantitative analyses of the midline injection sites

**Table 2** Cortical areas that contained labeled neurons after injections in area 10, and the percentages of the extrinsic labeled neurons they contained.

| Cortical area                                    | Midline injections |             |             | Lateral injections |             |                |             |             |
|--|--------------------|-------------|-------------|--------------------|-------------|----------------|-------------|-------------|
|  | Site 1             | Site 2      | Site 3      | Site 4             | Site 5      | Site 6         | Site 7      | Site 8      |
| 8b   | 0.5                | 0.4         | 1.2         | 6.5                | 0.1         | 0.4            | 0.2         | <0.1        |
| 9  | 3.7                | 6.6         | 15.9        | 9.3                | 4.1         | 3.0            | 13.0        | 1.9         |
| 46   | 14.8               | 21.0        | 23.8        | 35.2               | 6.6         | 7.8            | 13.8        | 27.5        |
| <b>Total DLPFC<sup>a</sup></b>                   | <b>18.9</b>        | <b>28.0</b> | <b>40.9</b> | <b>51.0</b>        | <b>10.8</b> | <b>11.3</b>    | <b>27.0</b> | <b>29.5</b> |
| 11   | 0.8                | 2.5         | 0.5         | 0.6                | 18.4        | 17.0           | 13.3        | 6.2         |
| 13   | 31.6               | 8.3         | 3.7         | 10.6               | 20.1        | 11.6           | 14.2        | 5.6         |
| OPal, OPro                                       | 0.4                | 0.5         | 0.2         | 0.4                | 1.3         | 0.3            | 0.6         | 0.1         |
| <b>Total OFC<sup>b</sup></b>                     | <b>32.8</b>        | <b>11.4</b> | <b>4.4</b>  | <b>11.6</b>        | <b>39.8</b> | <b>28.9</b>    | <b>28.2</b> | <b>12.0</b> |
| 12   | 14.2               | 3.5         | 2.0         | 10.7               | 7.0         | 25.0           | 26.0        | 42.0        |
| PrCO   | 0.8                | <0.1        | 0.1         | —                  | 1.4         | 0.1            | 0.5         | —           |
| <b>Total VLFC<sup>c</sup></b>                    | <b>15.1</b>        | <b>3.5</b>  | <b>2.1</b>  | <b>10.7</b>        | <b>8.4</b>  | <b>25.0</b>    | <b>26.5</b> | <b>42.0</b> |
| 14   | 7.0                | 14.6        | 4.8         | 6.3                | 33.5        | 20.6           | 4.1         | 0.4         |
| 24   | 0.7                | 0.2         | 0.2         | 0.4                | 0.5         | 0.1            | 5.5         | 3.1         |
| 25   | —                  | 0.2         | —           | —                  | <0.1        | —              | —           | —           |
| 32   | 1.5                | 4.3         | 19.0        | 9.5                | 1.4         | 6.2            | 3.2         | 5.7         |
| <b>Total MFC<sup>d</sup></b>                     | <b>9.1</b>         | <b>19.3</b> | <b>24.0</b> | <b>16.2</b>        | <b>35.4</b> | <b>26.9</b>    | <b>12.9</b> | <b>9.3</b>  |
| TAa  | 4.8                | 10.2        | 9.0         | 4.3                | 0.4         | 3.4            | 1.3         | 1.1         |
| TG   | 1.5                | 0.2         | 0.7         | —                  | 0.8         | <0.1           | —           | <0.1        |
| TS   | 7.2                | 13.3        | 6.3         | 1.3                | 2.0         | 2.0            | 0.2         | 0.3         |
| TPO  | 4.0                | 3.1         | 1.7         | 0.8                | 0.2         | 2.0            | 1.1         | 0.5         |
| PGa + IPa  | 3.8                | 1.1         | 0.1         | —                  | 0.4         | 0.2            | —           | 0.7         |
| TPt  | 0.3                | 0.7         | 0.2         | 0.4                | —           | —              | —           | 0.1         |
| TH + TL  | —                  | —           | 0.5         | —                  | —           | —              | —           | <0.1        |
| Parainsular                                      | 0.1                | 0.1         | 0.1         | 0.2                | 1.4         | 0.1            | —           | —           |
| <b>Total temporal association</b>                | <b>21.5</b>        | <b>28.7</b> | <b>18.6</b> | <b>7.0</b>         | <b>5.2</b>  | <b>7.7</b>     | <b>2.8</b>  | <b>2.8</b>  |
| Core (RT)  | —                  | 0.2         | —           | —                  | —           | —              | —           | —           |
| MB   | 0.2                | 0.1         | 0.2         | 0.5                | 0.2         | 0.1            | —           | —           |
| LB   | <0.1               | 0.5         | <0.1        | —                  | <0.1        | —              | —           | —           |
| Parabelt   | 1.0                | 5.8         | 1.4         | —                  | 0.1         | 0.1            | —           | —           |
| <b>Total auditory</b>                            | <b>1.2</b>         | <b>6.5</b>  | <b>1.6</b>  | <b>0.5</b>         | <b>0.3</b>  | <b>0.2</b>     | —           | —           |
| 23   | 0.2                | 0.5         | 1.6         | 2.0                | <0.1        | —              | 0.2         | 0.1         |
| 29 + 30  | 0.5                | 1.9         | 5.0         | 0.5                | <0.1        | <0.1           | 2.5         | 3.9         |
| Prostriata                                       | 0.4                | 0.3         | 1.8         | 0.5                | 0.1         | <0.1           | 0.2         | 0.2         |
| <b>Total PCC<sup>e</sup> and RSC<sup>f</sup></b> | <b>1.1</b>         | <b>2.7</b>  | <b>8.3</b>  | <b>3.0</b>         | <b>0.1</b>  | <b>&lt;0.1</b> | <b>2.8</b>  | <b>4.2</b>  |

Note: Boldface values represent the total percent distribution of extrinsic labeled neurons in main cortical sectors.

<sup>a</sup>Dorsolateral prefrontal cortex.

<sup>b</sup>Orbitofrontal cortex.

<sup>c</sup>Ventrolateral frontal cortex.

<sup>d</sup>Medial frontal cortex.

<sup>e</sup>Posterior cingulate cortex.

<sup>f</sup>Retrosplenial cortex.

are presented in Figures 4–6, and Table 2. With the exception of 2 isolated neurons in site 2, there were no connections with occipital or parietal areas. Instead, labeled neurons were located in the frontal (Fig. 3E–G), temporal (Fig. 3B,C) and posterior cingulate/retrosplenial regions (Fig. 3A). The main results of quantitative analyses were consistent across the 3 midline injection sites (Table 2).

Most connections (62.6–75.9% of the extrinsic cortical projections; Figs 4–6) originated in the frontal lobe. In the dorsolateral prefrontal cortex, area 46 consistently formed the main source of afferents to midline area 10 (14.8–23.8% of the labeled neurons; Fig. 3F,G), but large numbers of projecting neurons were also observed in area 9 (3.7–15.9%; Fig. 3G). Although they were observed in each site, projections from area 8b (Fig. 3F) accounted

for a much smaller percentage of the projecting neurons (0.4–1.2%). In the medial frontal cortex (Fig. 3G), areas 14 (4.8–14.6% of labeled neurons) and 32 (1.5–19.0%) formed the majority of projections, with most other afferents being located in area 24 (0.2–0.7%; Fig. 3F). Projection neurons within area 25 were only observed in site 2 (0.2%). In the orbitofrontal cortex labeled neurons in area 13 (3.7–31.6%) consistently outnumbered those in area 11 (0.5–2.5%). Smaller numbers of projection neurons (0.2–0.5%) were also found in the orbital periallocortical area (OPal; Fig. 3D), near the transition with the temporal lobe. Finally, projection neurons (2.0–14.2% of the extrinsic label) were observed in area 12 of the ventrolateral prefrontal cortex, within which distinct rostral and caudal clusters of labeled cells were typically observed (Figs 4–6). Further caudally along the lateral margin

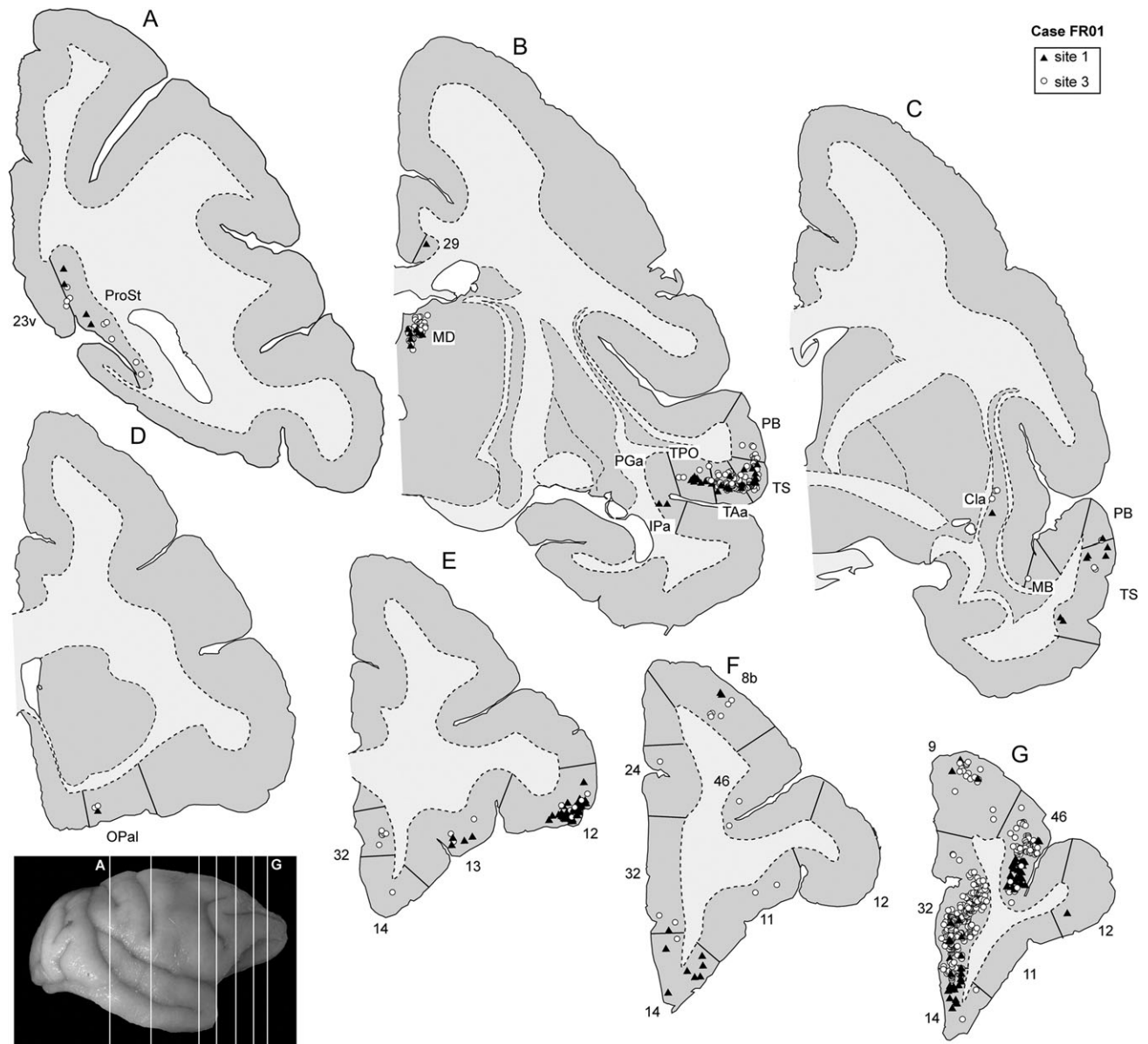


**Figure 3.** Representative coronal sections (A–G) showing the location of labeled neurons following 2 injections in animal FR01. The level of the sections is indicated in the photograph shown on the bottom left. The black triangles represent neurons labeled with the tracer FR, and the white circles represent FE-labeled neurons. Numerical designations refer to cytoarchitectural areas according to Cruz-Rizzolo et al. (2011) and Kobayashi and Amaral (2000). The designations IPa, PGa, TAa, TPO, and TS derive from studies by the Pandya group (see Petrides and Pandya 2007, for a summary). 12l: area 12, lateral subdivision; 12o, area 12, orbital subdivision; 23 v, area 23, ventral subdivision; Cla, claustrum; MD, medial dorsal thalamic nucleus; OPal, orbital periallocortex; PB, parabelt auditory cortex; ProSt, area prostriata.

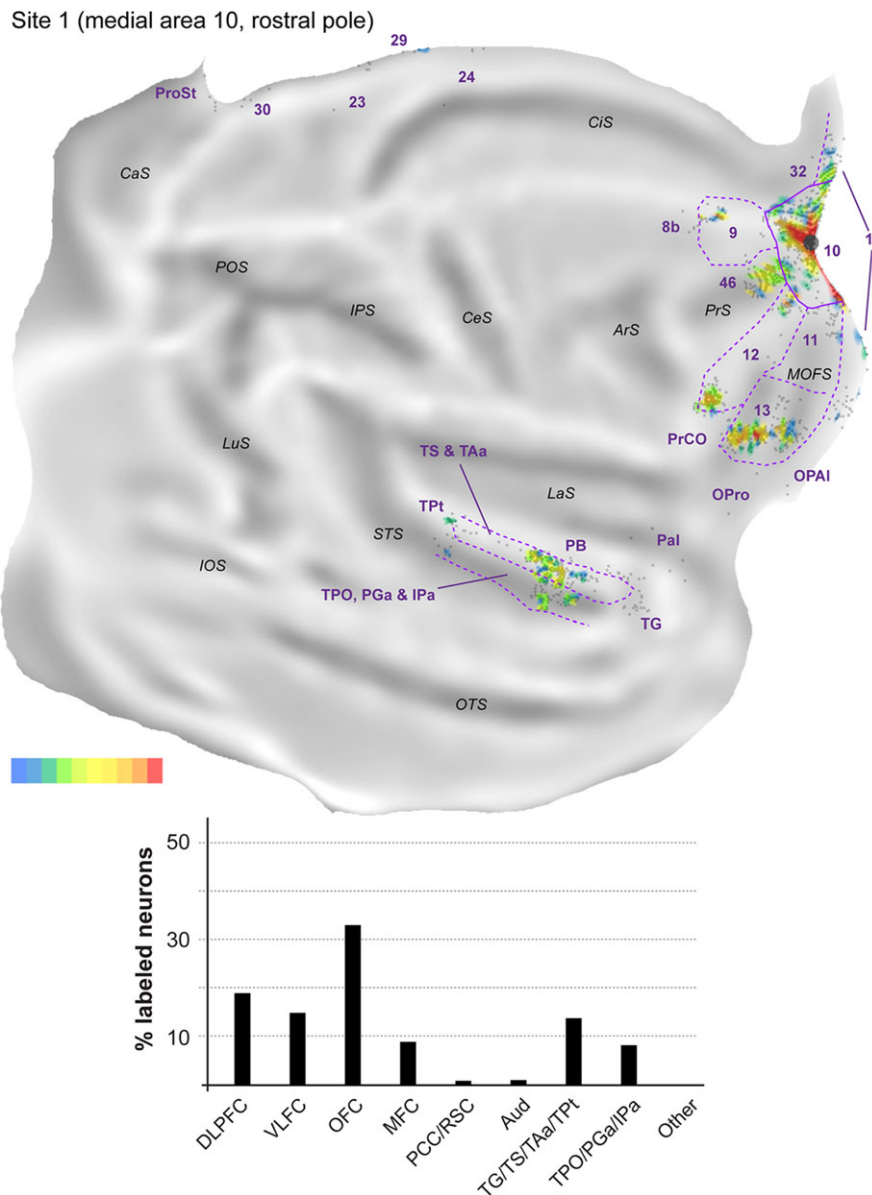


**Figure 4.** Top: 2D “unfolded” reconstruction of the cerebral cortex in animal FR01, showing the pattern of label resulting from an injection of FR in area 10 (site 1). Large aggregations of labeled neurons are indicated by color, as a percentage of the maximum density observed (bottom right scale; red = 91–100% of the maximum density across all layers, blue  $\leq$ 10% of the maximum density). Gray points represent individual neurons. Black circles indicate the centers of the injection sites. ArS, arcuate sulcus; CaS, calcarine sulcus; CeS, central sulcus; CIS, cingulate sulcus; IOS, inferior occipital sulcus; IPS, intraparietal sulcus; LaS, lateral sulcus; LuS, lunate sulcus; MOFS, medial orbital frontal sulcus; OTS, occipito-temporal sulcus; POS, parieto-occipital sulcus; PrS, principal sulcus; STS, superior temporal sulcus. **Bottom:** Summary of the percentages of extrinsic projection neurons labeled in different parts of the cerebral cortex (see Table 2 for details). DLPFC, dorsolateral prefrontal cortex (areas 8b, 9, 46); VLFC, ventrolateral frontal cortex (subdivisions of area 12, and precentral opercular cortex, PrCO); OFC, orbitofrontal cortex (areas 11, 13, OPal, and OPro [orbital preoccipital]); MFC, medial frontal cortex (areas 14, 24, 25, and 32); PCC/RSC, posterior cingulate cortex and retrosplenial cortex (areas 23, 29, 30, and prostriata); Aud, auditory cortex (rostrottemporal [RT] core, lateral and MB, and parabelt areas); TG/TS/TAa/TPT, subdivisions of the superior temporal auditory association cortex; TPO/PGa/IPa, subdivisions of the superior temporal polysensory cortex.

of the frontal lobe, the precentral opercular area (PrCO) contained scattered labeled neurons (<0.1–0.8%). Overall, site 1, with the injection closest to the apex of the frontal pole, resulted in high percentages of labeled cells in the orbital and ventrolateral prefrontal areas, but these projections decreased in relative strength with progressively more posterior injections (sites 2 and 3; see Figs 4–6).

Outside the frontal lobe, only a few cortical areas formed projections to midline area 10. In the temporal lobe, projections originated primarily from the superior temporal gyrus auditory

association cortex (Baylis et al. 1987; Colombo et al. 1996). Most of this label concentrated around the ventral part of the superior temporal gyrus (area TS) and dorsal lip of the superior temporal sulcus (area TAa; see Fig. 3B,C), with these auditory–visual association areas (Baylis et al. 1987) forming projections of approximately equal strength in each site (6.3–13.3% and 4.8–10.2%, respectively). The projections from TS and TAa were not uniformly distributed across these areas, suggesting that they may have subdivisions, some of which show specific connectivity with the frontal pole. Sparser connections from putative auditory



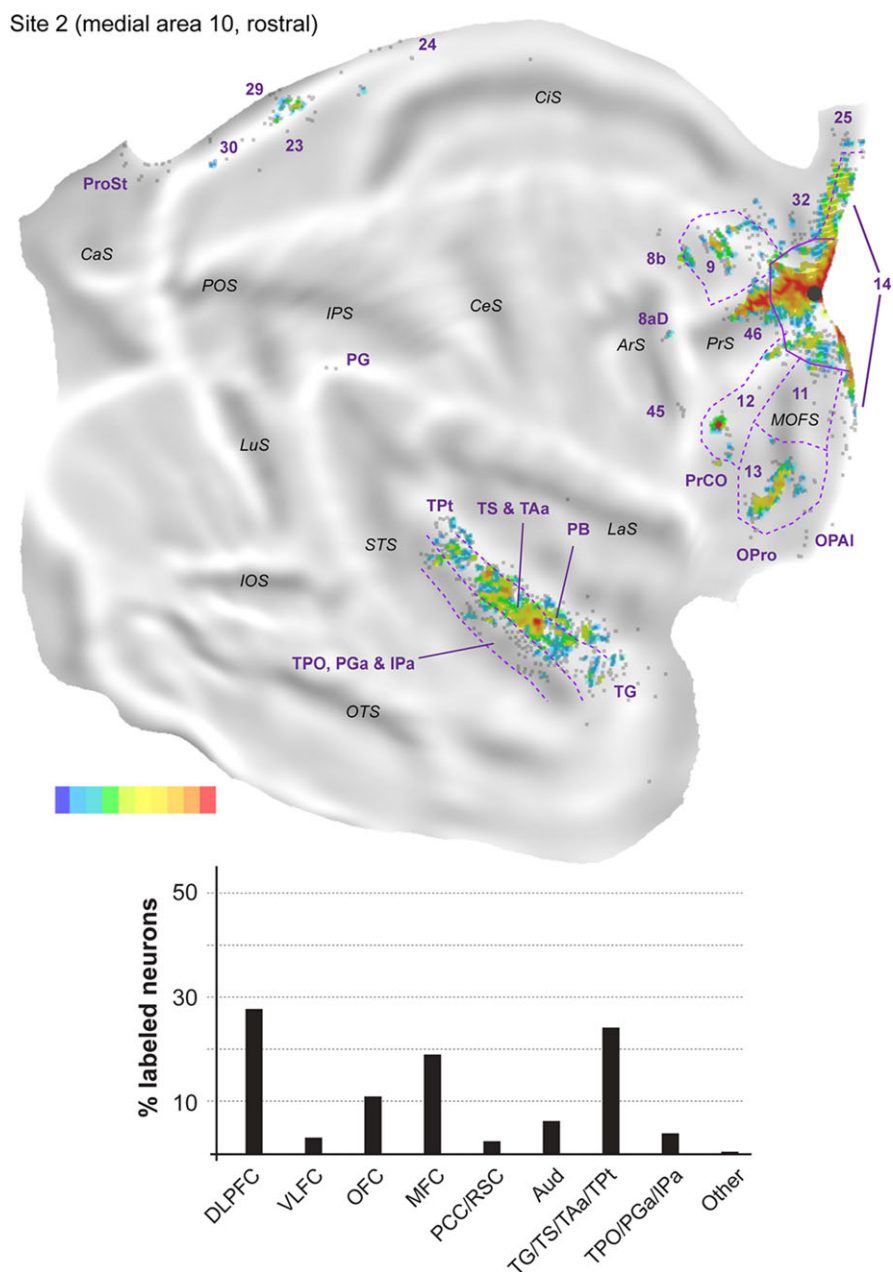


**Figure 5.** Top: “Unfolded” reconstruction of the cerebral cortex in animal FR02, showing the pattern of label resulting from an injection of FE (site 2). Bottom: Summary of the percentages of extrinsic projection neurons labeled in different parts of the cerebral cortex. Conventions as for Figure 4.

association or polysensory areas (Tranel et al. 1988; Munoz-Lopez et al. 2010) originated in area TPt (0.2–0.7%), in the temporal pole cortex (area TG; 0.2–1.5%) and, less prominently, in the parainsular cortex (~0.1% of the labeled neurons, in each site). In addition, each of the midline injections resulted in labeled neurons in unimodal auditory areas. Most of these cells were located in the parabelt (1.0–5.8% of the extrinsic projections to area 10), although isolated neurons were also found in the lateral and MB areas (0.2–0.6%) and, in site 2, in the rostrotemporal (RT) core area (see also Reser et al. 2009).

Polysensory areas in the dorsal bank and fundus of the superior temporal sulcus formed a second source of temporal lobe projections to midline area 10. Clusters of labeled neurons were observed in areas TPO, PGa, and IPa (Fig. 3B). Most of the labeled neurons were located within the borders of TPO (1.7–4.0%), with

PGa and IPa together accounting for an additional 0.1–3.8% of the projection neurons. Finally, the caudal-most midline injection (site 3) revealed labeled neurons in the medial temporal lobe (areas TL and TH; Fig. 6).

The posterior cingulate and retrosplenial regions formed the final source of afferents to medial area 10 (Fig. 3A,B). Projections from the internal and ventral subdivisions of area 23 (0.2–1.6% of the labeled projection neurons), area prostriata (0.3–1.8%) and pericallosal areas 29 and 30 (0.5–5.0%) were present in each site, but were most numerous in site 3.

### Injections in Lateral Area 10

The remaining 5 injections in area 10 are referred to here as “lateral injections” for convenience, even though they encompassed

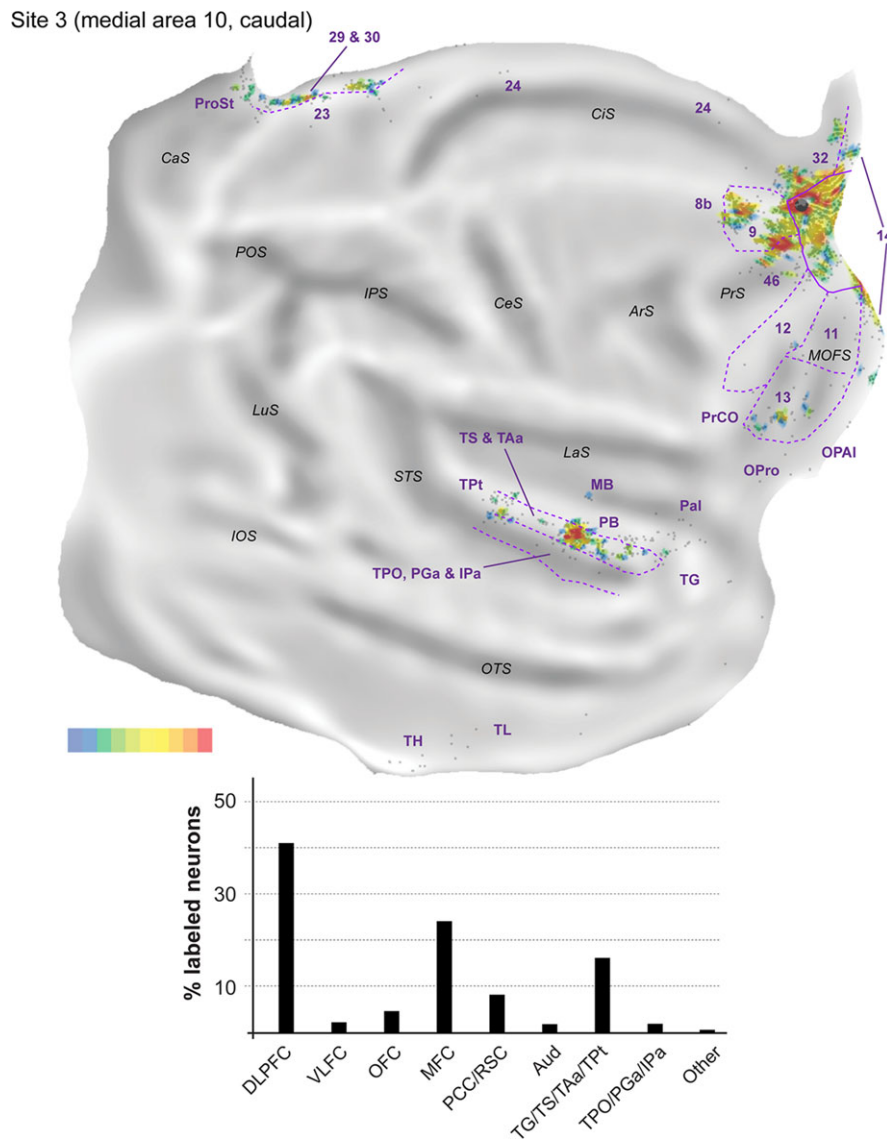


**Figure 6.** Top: “Unfolded” reconstruction of the cerebral cortex in animal FR01, showing the pattern of label resulting from an injection of FE (site 3). Bottom: Summary of the percentages of extrinsic projection neurons labeled in different parts of the cerebral cortex. Conventions as for Figure 4. TH, TL: cytoarchitectural areas, defined according to the criteria described by Blatt et al. (2003) in the macaque.

various locations. As a group they differ in important ways from the midline injections, as detailed below. Figure 7 shows the distribution of labeled neurons following 2 of these injections (sites 4 and 5) in animal FR01. Comparison with Figure 3 demonstrates that the locations of clusters of neurons that projected to lateral area 10 overlapped extensively with those revealed by midline injections. However, in lateral injection sites (Figs 8–12), long-range extrinsic projections were relatively de-emphasized, with frontal lobe afferents accounting for 89.0–94.5% of the labeled neurons outside area 10. Although the distribution of labeled neurons in the superior temporal association cortex was restricted in site 7 (Fig. 11), possibly due to the small extent of the injection and lack of involvement of the infragranular layers, quantitative analyses based on the percentages of labeled neurons in different areas provided results that were consistent with those revealed by other injections in lateral area 10 (Table 2). Likewise, results from site 8 (Fig. 12), which had possible involvement of the most rostral part of area 121,

were in agreement with those of other injections in this group, with the only major differences being the presence of a small patch of labeled neurons in the inferior parietal lobule (area PG), which accounted for 0.3% of the extrinsic projection neurons, and another in ventrolateral frontal area 45 (<0.1%).

The proportion of labeled neurons in dorsolateral prefrontal areas was highest in site 4 (Fig. 8, Table 2), an injection restricted to the dorsal surface of rostral area 10. Similar to midline injections, projections from area 46 (6.6–35.2% of the extrinsic projections) outnumbered those from areas 8b (<0.1–6.5%) and 9 (1.9–13.0%) in every lateral injection site. However, unlike in midline injections, in the orbitofrontal cortex the proportion of afferents from areas 11 (0.6–18.4%) and 13 (5.6–20.1%) was approximately balanced in most sites. The outlier in this respect was site 4, which resembled midline injections in showing a clear predominance of area 13 projections (Table 2). Projections from the orbital insular cortex (0.1–1.3% of labeled cells) originated not only in the orbital

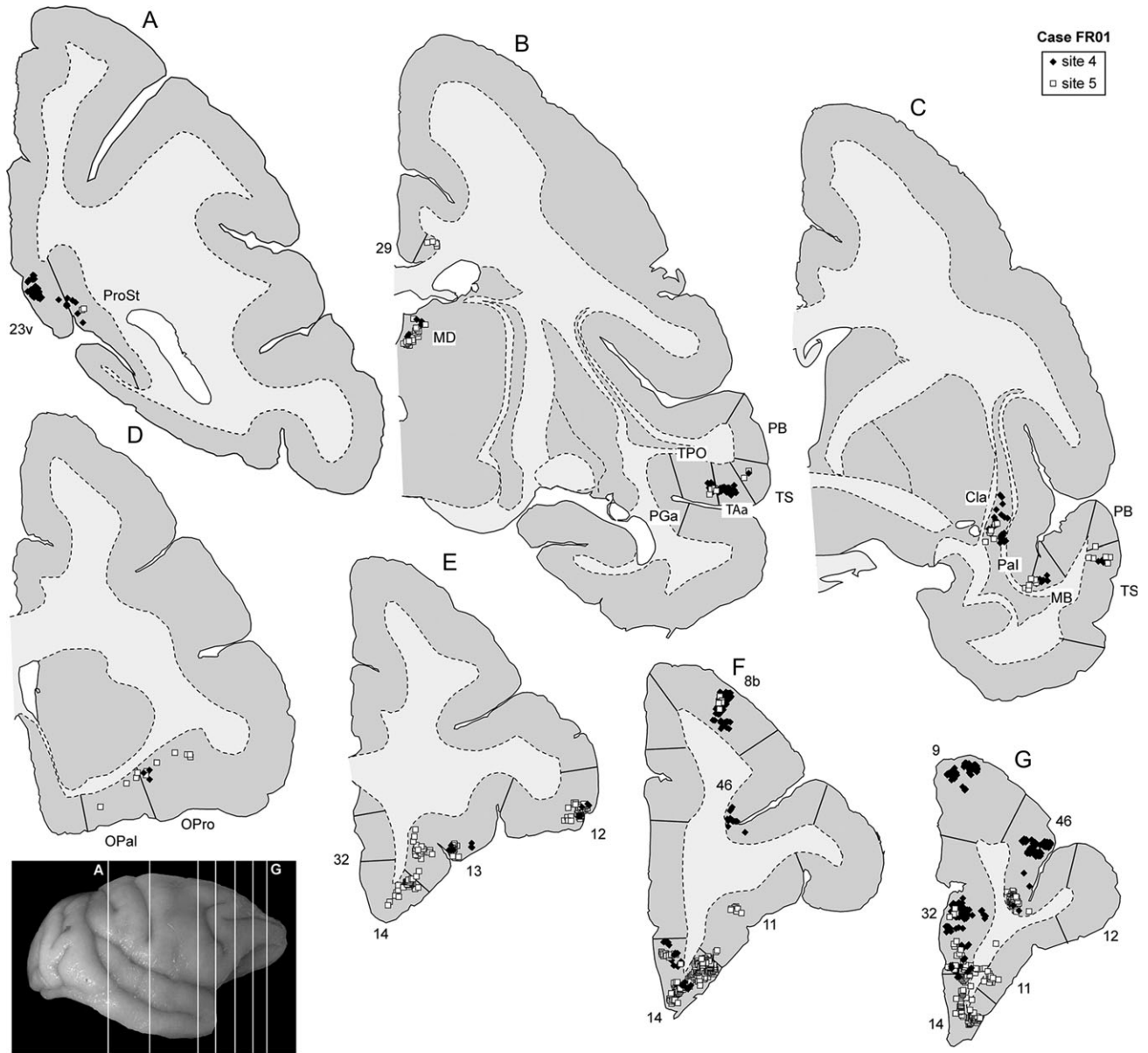


**Figure 7.** Representative coronal sections (A–G) showing the location of labeled neurons following 2 injections in animal FR01. The level of the sections is indicated in the photograph shown on the bottom left. The white squares represent neurons labeled with the tracer FB, and the black diamonds represent DY-labeled neurons.

pericallocortex (OPal) but also more laterally, in the orbital preocortex (OPro).

The percentages of labeled neurons in the medial frontal cortex were similar to those observed following midline injections, with the bulk of the label again located in areas 14 (0.4–33.5% of the extrinsic afferents) and 32 (1.4–9.5%). The highest proportions of labeled neurons in medial areas were observed in sites 5 and 6 (injections which involved the ventral aspect of the frontal pole), mostly due to dense labeling of area 14, whereas sites 7 and 8 (the most lateral injections) were distinguished by the high percentage of labeled neurons in anterior cingulate area 24 (5.5 and 3.1% of the projecting neurons; Table 2). Labeled neurons in area 12 (7.0–26.0%; this range excludes site 8, due to the likelihood that some of the labeled cells in area 12 corresponded to intrinsic connections) were located in the same regions that projected to the midline injection sites, that is, the rostral and caudal portions of this area, avoiding the middle part. Projections from PrCO to

lateral area 10 were observed in sites 5, 6, and 7 (<0.1–1.4% of the extrinsic label).

As highlighted above, the main difference revealed by comparing the results of injections in the midline versus lateral group was the paucity of long-range projections to the latter. Projections from cytoarchitectural areas TS (0.3–2.0% of the labeled neurons), TAA (1.1–4.3%), and TPO (0.2–2.0%) were observed in every case, but those from PGa/IPa were only evident in sites 5, 6, and 8, and were very sparse (0.2–0.7%). Temporal pole (area TG) projections were also only evident in sites 5, 6, and 8, those from TPt only in sites 4 and 8, and those from the parainsular cortex in sites 4, 5, and 6 (Table 2). Unimodal auditory projections from the MB and parabelt were only detected in sites 4, 5, and 6, and consisted of isolated neurons (0.2–0.5% of the extrinsic afferents). The absence of any label in auditory cortex in sites 7 and 8 (despite the large number of labeled neurons elsewhere in the latter case; Table 1)

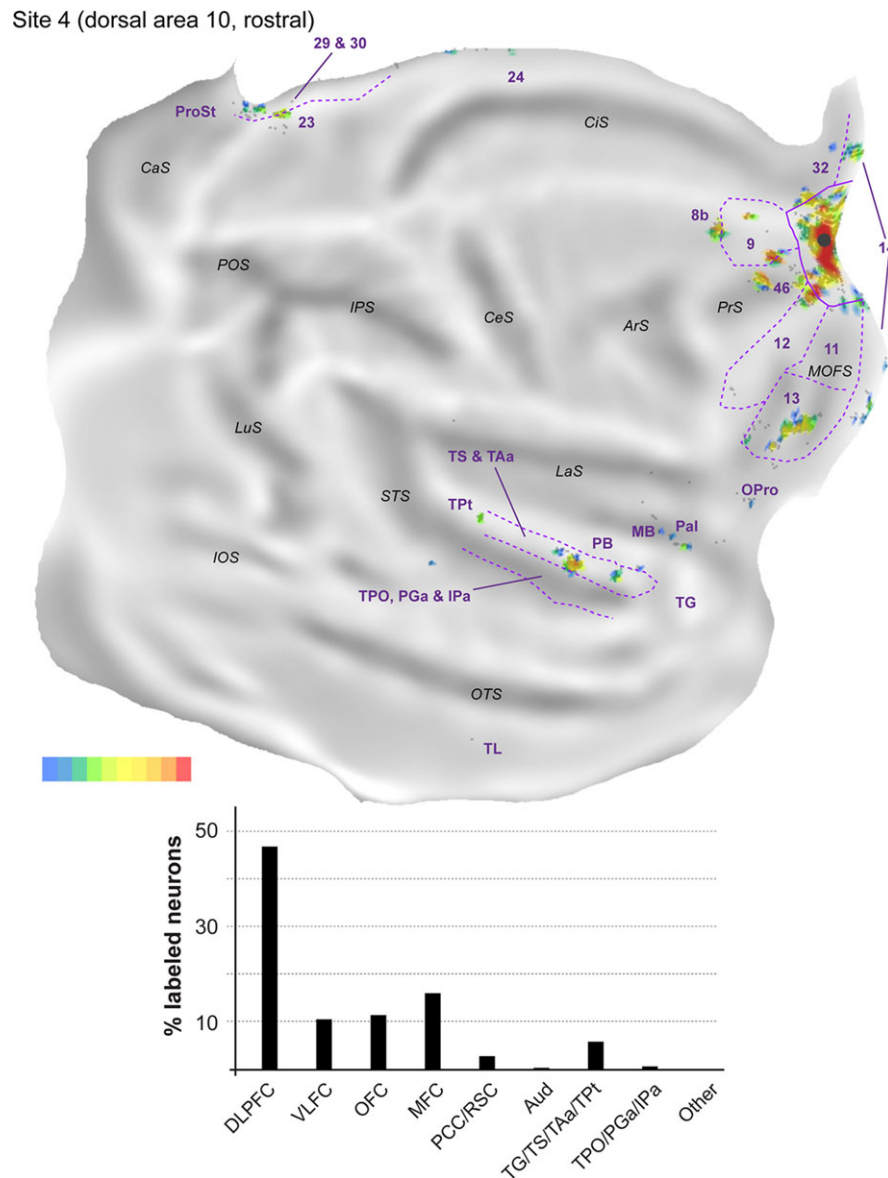


**Figure 8.** Top: “Unfolded” reconstruction of the cerebral cortex in animal FR01, showing the pattern of label resulting from an injection of DY (site 4). Bottom: Summary of the percentages of extrinsic projection neurons labeled in different parts of the cerebral cortex. Conventions as for Figure 4.

reinforces the notion of a mediolateral gradient in area 10, with auditory projections preferentially targeting its medial aspect.

Further caudally, area prostriata contained label following each of the lateral injections, but this projection was sparser (<0.1–0.5%) than that observed following midline injections. Projections from areas 23, 29, and 30 were also observed in the majority of lateral injection sites, with site 8 in particular standing out for its robust set of retrosplenial projections (Figs 12).

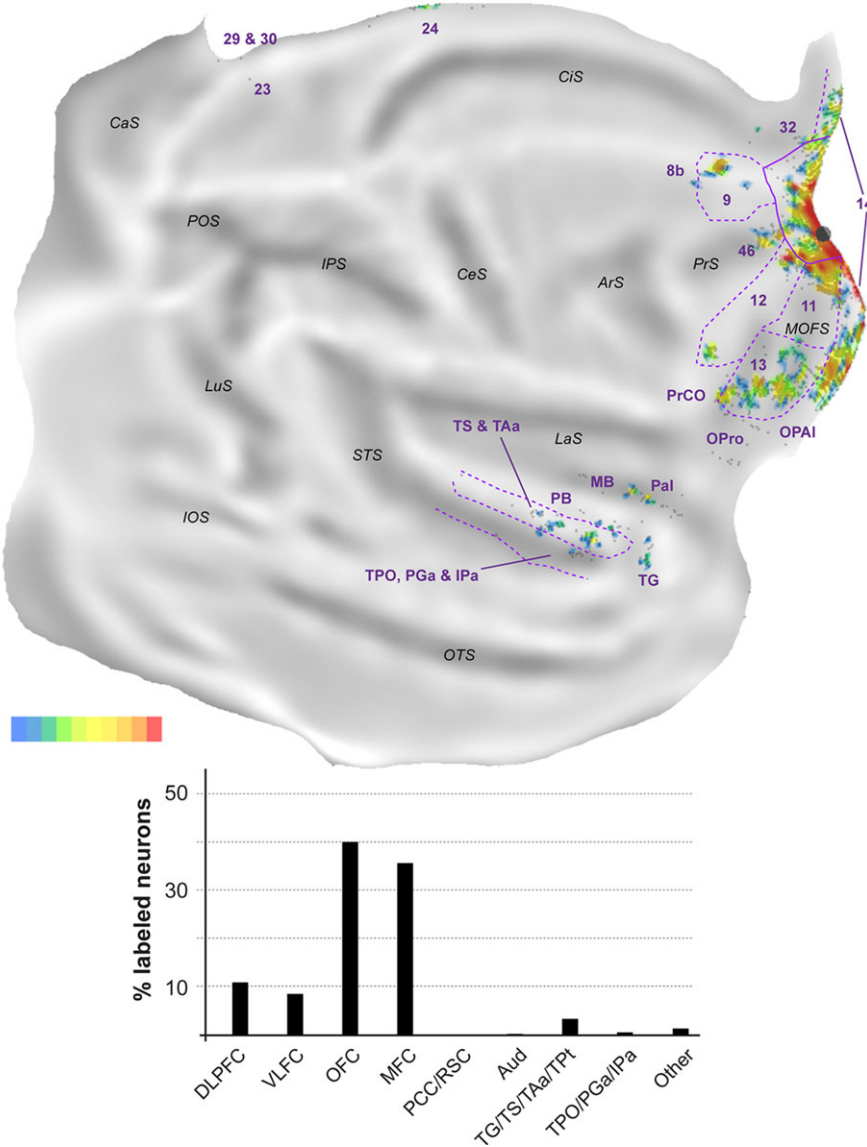
### Injections Caudal to Area 10 Revealed Different Patterns of Connections

Figure 13 illustrates the results of the injections placed in areas caudal to area 10. Site 9, which was an injection in the ventral (orbital) surface of rostral area 12 (Fig. 13, Top), revealed a markedly different pattern of projections from the temporal and midline regions. Rather than the superior temporal gyrus, the main temporal projections originated from the rostral part

of visual association area TE, on the ventral bank of the superior temporal sulcus and inferior temporal gyrus, in addition to sparse input from polysensory areas in the fundus of the superior temporal sulcus (PGa/IPa). Moreover, the label was shifted dorsally along the midline cortex, with greater involvement of areas 23 and 24, and no projections from areas 29 and 30. In the medial prefrontal cortex, area 32, which formed consistent projections to area 10, was devoid of label, whereas in the dorsolateral prefrontal cortex clear patches of labeled neurons were found in areas 45 and PrCO.

Site 10, an injection in lateral area 9 (Fig. 13, Bottom), contrasted with those in area 10 in the absence or paucity of projections from areas 14 and area 32, and from the caudal orbitofrontal region (with the exception of a small cluster in area 13). This injection also resulted in multiple, strong projections from the cingulate region (including putative homologs of areas PGm, 31, PEci, and subdivisions of areas 23 and 24), which were not seen following area 10 injections.

Site 5 (lateral area 10, rostral and ventral)



**Figure 9.** Top: “Unfolded” reconstruction of the cerebral cortex in animal FR01, showing the pattern of label resulting from an injection of FB (site 5). Bottom: Summary of the percentages of extrinsic projection neurons labeled in different parts of the cerebral cortex. Conventions as for Figure 4.

The transitions in connectional patterns revealed by these cases reflect those previously observed in macaques and marmosets (Barbas 1988; Carmichael and Price 1995; Petrides and Pandya 2007; Burman et al. 2011b; Medalla and Barbas 2014; Saleem et al. 2014; Passarelli et al. 2017), reaffirming the essential similarity in organization of connections across rostral frontal areas in New World (*Cebus*) and Old World (*Macaca*) primates.

## Discussion

This study was motivated by 2 interrelated questions. First, do monkeys show evidence of anatomical subdivisions of area 10, which could be seen as precursors of the lateral and medial frontopolar areas proposed for the human brain? Second, does the pattern of connections of area 10 in *Cebus* more closely resemble that described in the marmoset, a species with which it shares a more recent common ancestor (Fig. 14), or that in the more distantly related macaque, which has similar brain morphology?

Our results support the view that area 10, as a whole, can be defined by its pattern of afferents. A highly specific set of cortical areas was found to send projections throughout the extent of area 10, and this pattern differed from those revealed by injections in adjacent areas 9 and 12. Overall, what is known about the functions of the frontal areas that form the sources of cortical projections to area 10 suggests that this is a site of convergence of information that pertains to executive control of cognitive function, including various aspects of working memory (spatial, rule-based), object categorization, assignment of value, and motivation (e.g., Jacobson and Trojanowski 1977; Barbas et al. 1999; Cavada et al. 2000; Saleem et al. 2008; Mansouri et al. 2015). At the same time, there are no connections from areas directly involved in motor control or preparation, or areas that correspond to low hierarchical levels of sensory processing. The most immediate visual projections originate from the somewhat enigmatic area prostriata, in retrosplenial cortex (Yu et al. 2012; Mikellidou et al. 2017), whereas auditory projections (largely, to medial area 10)

## Site 6 (lateral area 10, rostral and ventral)

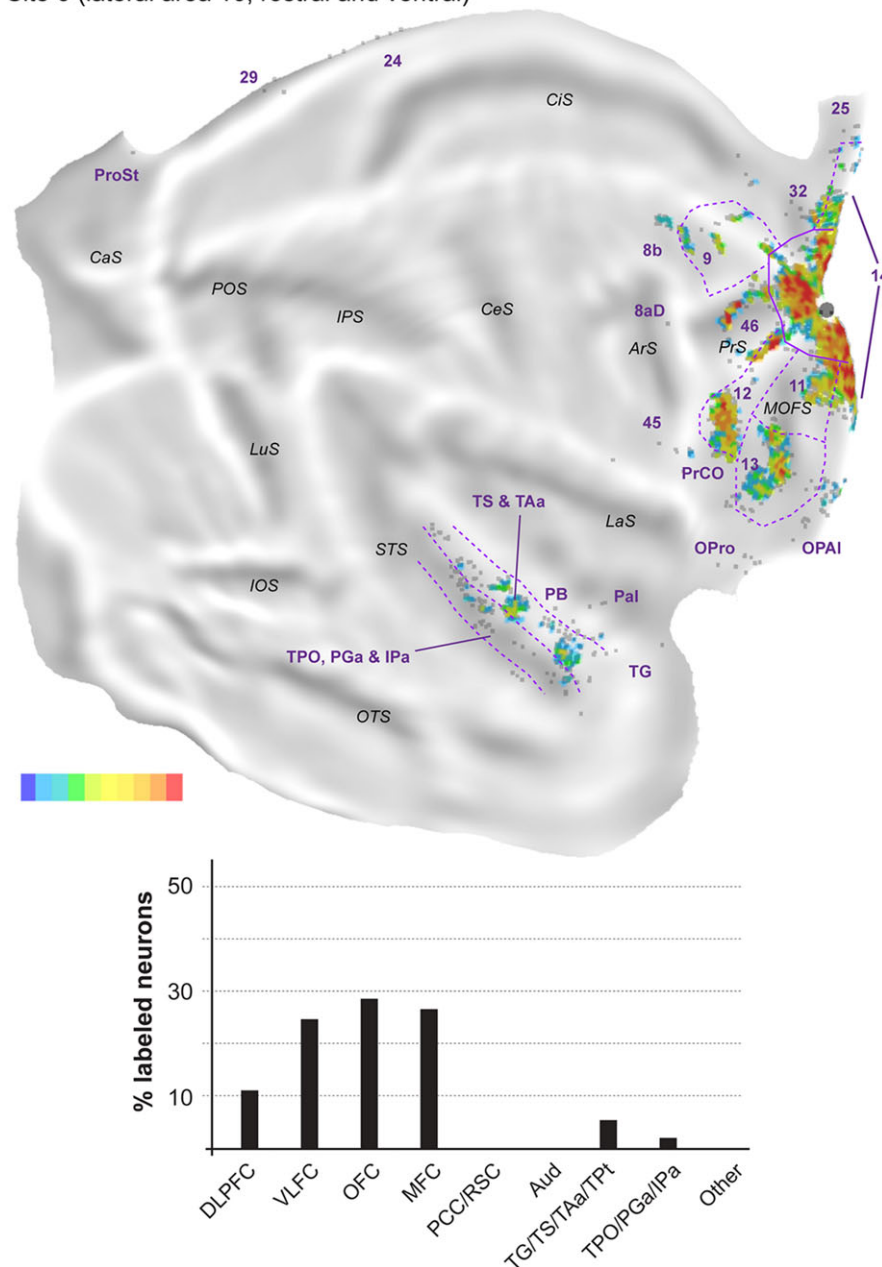


**Figure 10.** Top: “Unfolded” reconstruction of the cerebral cortex in animal FR02, showing the pattern of label resulting from an injection of FB (site 6). Bottom: Summary of the percentages of extrinsic projection neurons labeled in different parts of the cerebral cortex. Conventions as for Figure 4.

originate primarily in the parabelt cortex (see also [Hackett et al. 1999](#); [Medalla and Barbas 2014](#); [Kajikawa et al. 2015](#)). Most connections from the temporal lobe stem from polysensory areas of the superior temporal gyrus and upper bank of the superior temporal sulcus (TS, TAa, TPO, PGa, and IPa; [Baylis et al. 1987](#)).

#### Are There Subdivisions in Area 10 of the *Cebus* Monkey?

Despite the general uniformity of the major connections to area 10, our results demonstrate the presence of a gradient of connections superimposed on this pattern, particularly in the mediolateral dimension, whereby the majority of high-order auditory association and polysensory inputs target the medial

aspect of area 10. Other anatomical gradients (e.g., in the dorso-ventral dimension) were also suggested by the data. Thus, the apparent uniformity of area 10 accommodates subtle variations in inputs, which may have provided the initial basis for differentiation into areas in parallel with the expansion of the frontal pole in human evolution.

A retrospective analysis of the results obtained in marmosets ([Burman et al. 2011b](#)) and macaques ([Saleem et al. 2014](#)) reveals parallels with the current findings. For example, in [Saleem et al. \(2014\)](#) tracer injections near the midline (their sites OM69 and OM77) revealed stronger connections with the parabelt, medial temporal lobe, cingulate and retrosplenial areas, in comparison with a lateral injection (their site OM19), whereas in Burman

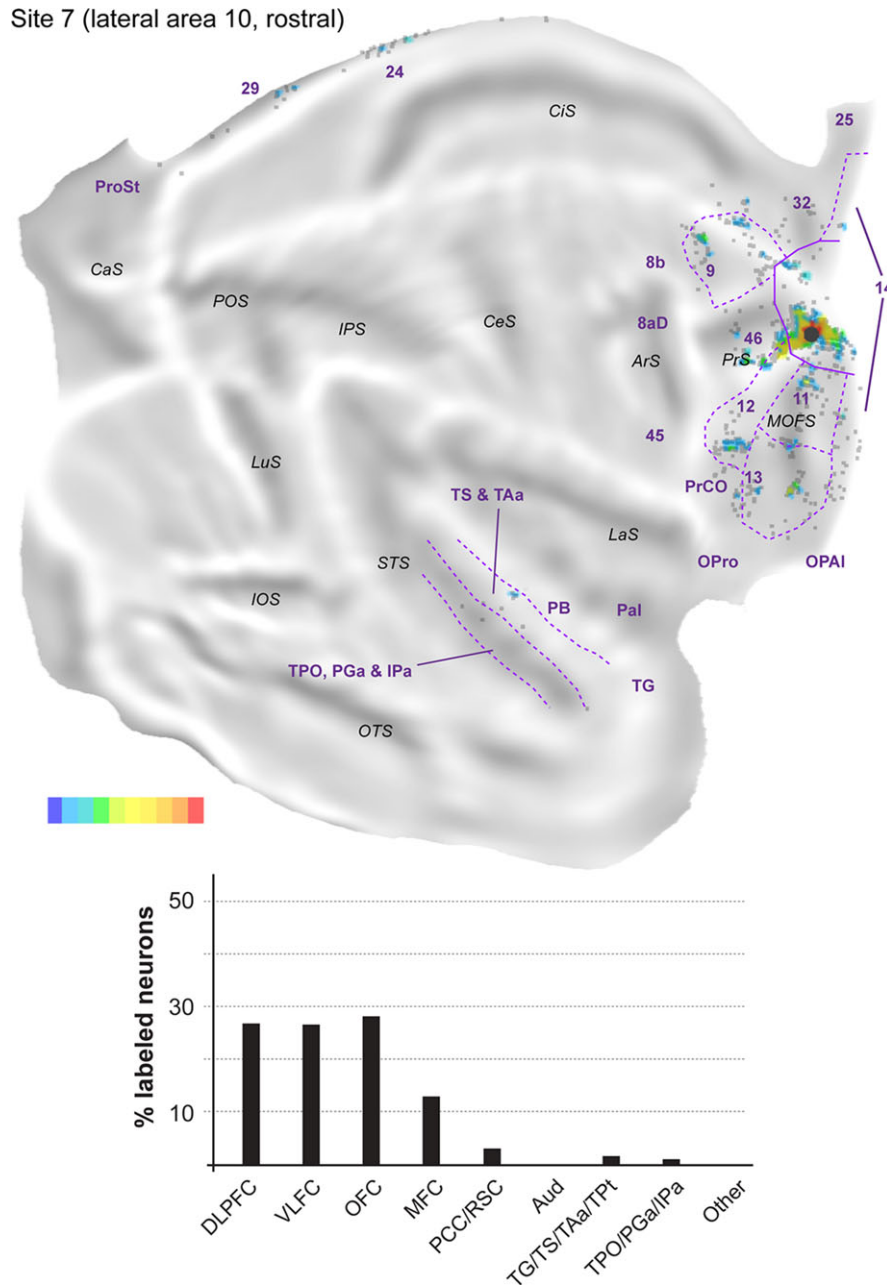


**Figure 11.** Top: “Unfolded” reconstruction of the cerebral cortex in animal FR02, showing the pattern of label resulting from an injection of FR (site 7). Bottom: Summary of the percentages of extrinsic projection neurons labeled in different parts of the cerebral cortex. Conventions as for Figure 4.

et al. (2011b) the highest proportion of auditory cortex label was also observed following an injection parallel to the midline (their site CJ73FR). Noninvasive imaging studies have also suggested differences between lateral and medial subdivisions of the human frontopolar cortex (Liu et al. 2013; Neubert et al. 2014; Moayedi et al. 2015; Orr et al. 2015). Importantly, the human lateral frontopolar cortex is reported to have reduced functional connectivity with the superior temporal gyrus and retrosplenial cortex in comparison with the medial frontopolar cortex, an observation that aligns well with the present findings in monkeys.

One of the best-established models of the frontopolar cortex proposes distinct functions for its medial and lateral

subdivisions in monitoring action outcomes versus cognitive branching (Koechlin 2011). More recently, this framework has been expanded to accommodate the hypothesis that the medial frontopolar cortex has a function in assessing the relative value of current versus alternative behaviors according to changes in the environment (Mansouri et al. 2017), whereas the lateral subdivision performs the ongoing monitoring of multiple goals or mental processes in parallel, and promotes the allocation of cognitive resources between these as required (a function that underpins cognitive branching). The present results do not necessarily challenge the view that the human lateral frontopolar cortex contains a unique area, which has no functional equivalent in nonhuman primates (Neubert et al.

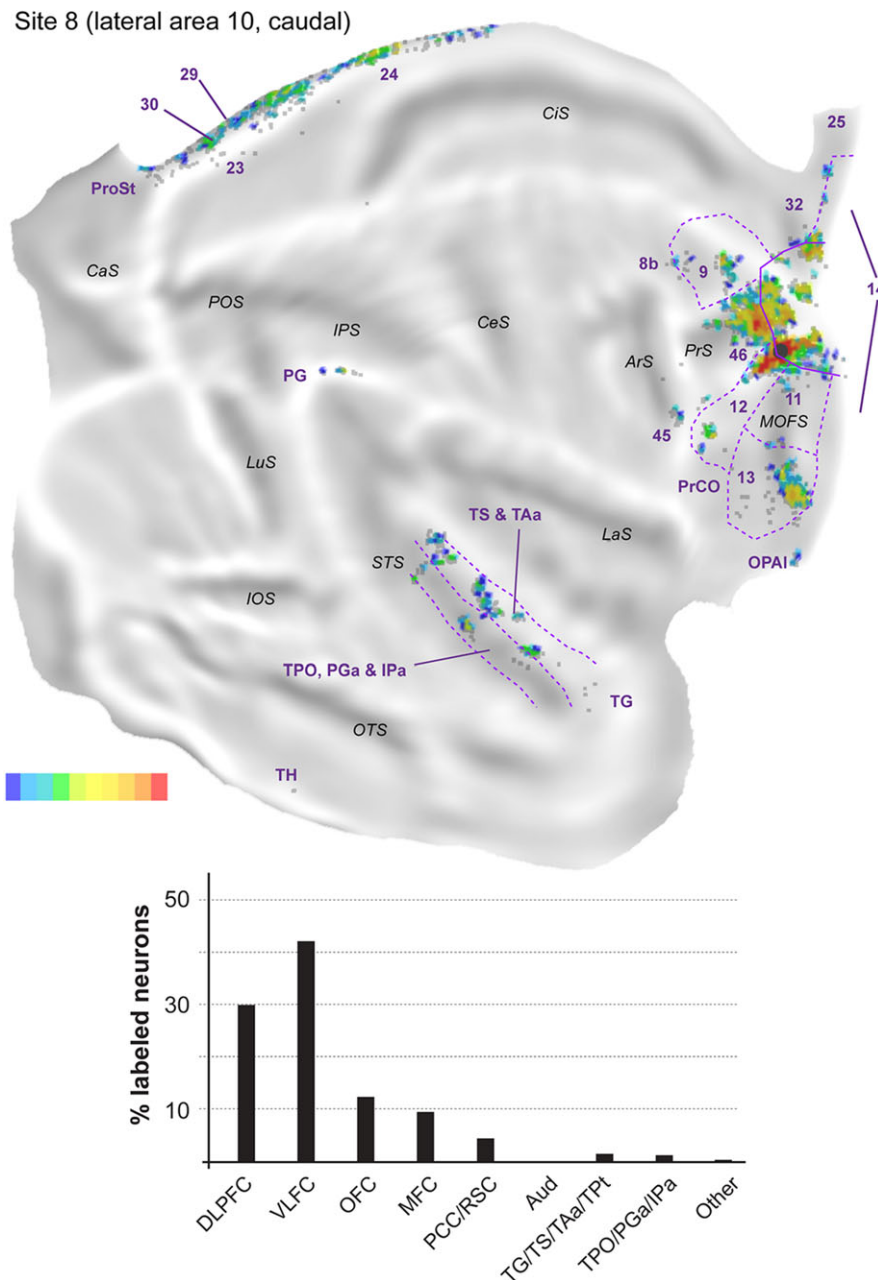


**Figure 12.** Top: “Unfolded” reconstruction of the cerebral cortex in animal FR02, showing the pattern of label resulting from an injection of DY (site 8). Bottom: Summary of the percentages of extrinsic projection neurons labeled in different parts of the cerebral cortex. Conventions as for Figure 4.

2014; Mansouri et al. 2017). However, they do indicate that the clearer segregation observed in humans may have an evolutionary predecessor. The observations that the midline sector of area 10 receives a high proportion of afferents from the temporal sensory association cortex is compatible with a proposed role in monitoring the environment for significant changes which may require a change in behavioral focus. Conversely, the fact that the lateral part of area 10 receives the overwhelming majority (~90%) of its afferents from other frontal association areas aligns well with a possible role in the management of cognitive resources across concurrent tasks. The notion that the frontopolar cortex has changed from a gradient-like organization to one where segregated areas exist, in parallel with changes in overall brain mass, is in agreement with current

views of the mechanisms of cortical evolution (Rosa and Tweedale 2005; Striedter 2005; Krubitzer 2009).

### Comparison with the Macaque Monkey

Old World macaques are the primate genus for which most cortico-cortical connectivity information is available. Following from Jacobson and Trojanowski (1977), subsequent studies have illustrated data from retrograde tracer injections in different portions of area 10 (Barbas et al. 1999; Cavada et al. 2000; Saleem et al. 2008; Medalla and Barbas 2014). As in *Cebus*, the primary projections to macaque area 10 originate only in the rostral dorsolateral, ventrolateral, orbital and medial subdivisions of the frontal cortex, in the superior



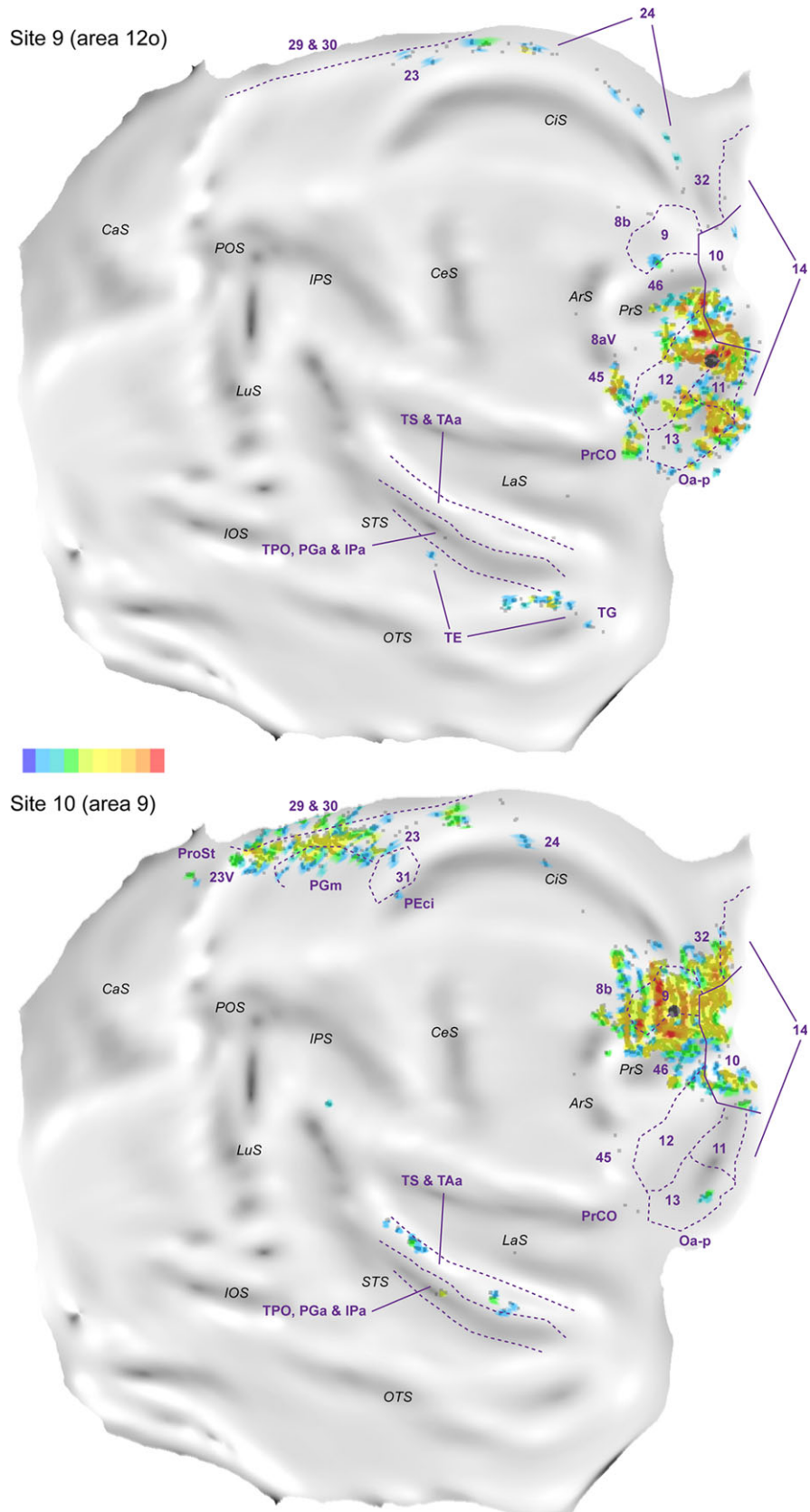


**Figure 13.** “Unfolded” reconstruction of the cerebral cortex in animal FR04, showing the pattern of label resulting from an injection of DY in area 12 (site 9) and an injection of FB in area 9 (site 10). Conventions as for Figure 4. TE, PGm, 31 and PEci refer to areas defined using the same criteria used in the macaque cortex (e.g., Passarelli et al. 2017).

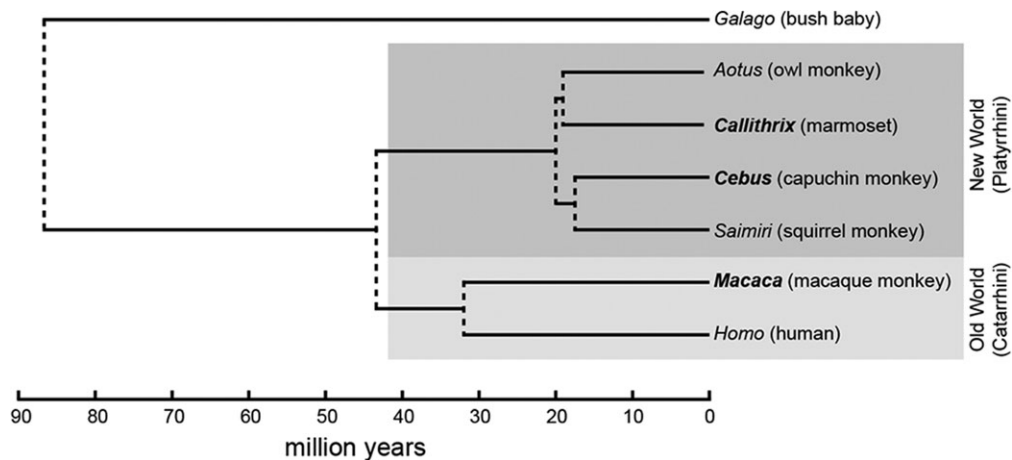


**Figure 14.** Cladogram showing the phylogenetic relationships between some of the primate species most commonly used in neuroscience research, derived from genomic sequences (Perelman et al. 2011). This representation indicates the most likely times of divergence between lineages leading to present-day genera (right). New World monkeys (including *Cebus* and *Callithrix*, the marmoset) are part of a monophyletic group (dark gray) whose last common ancestor was approximately 20 million years ago, whereas humans and macaques belong to another monophyletic group (Old World “monkeys”, light gray) which had a common ancestor approximately 32 million years ago. The common ancestor of all present-day monkeys, apes, and humans existed approximately 43 million years ago.

temporal gyrus and sulcus, and in pericallosal areas. When judged relative to the sulcal morphology, the patterns in *Cebus* and *Macaca* appear identical.

It is much harder to judge whether there are any systematic differences at the level of fine detail, given that reports on the afferents of macaque area 10 are each based on few cases, and differ in methodology (e.g., different schemes for parcellation of cortical areas, variations in the location of injections, and the sporadic use of quantification). For example, our results align well with those of Cavada et al. (2000) and Saleem et al. (2014) in suggesting that orbitofrontal areas 11 and 13 both form substantial projections to area 10; in contrast, Barbas et al. (1999) report that orbitofrontal afferents originate almost exclusively from area 11. Considering the available information we conclude that any differences between *Cebus* and macaque monkeys are likely to be minor, if present at all.

### Comparison with the Marmoset Monkey

*Cebus* and marmoset (*Callithrix*) monkeys derive from a common New World primate ancestor species (Fig. 14), which diverged from the group that led to Old World monkeys 40–45 million years ago (Steiper and Young 2006; Chatterjee et al. 2009; Perelman et al. 2011; Perez et al. 2012). The New World monkey lineages leading to present-day *Cebus* and *Callithrix* did not diverge until much later (~20 million years ago; Perelman et al. 2011). Thus, despite the very different body (and brain) masses, there is much greater genetic similarity between *Cebus* and marmoset monkeys, than between either of these species and macaques.

In an earlier study, Burman et al. (2011b) reported that the main projections to area 10 in the marmoset came from the same areas that form projections in macaques, but that the marmoset brain also showed evidence of a more expansive network of afferents. In an attempt to minimize the subjectivity in this comparison, in Figure 15 we have plotted composite views of all the neurons that form connections to area 10 in *Cebus* and marmoset monkeys, based on coregistration of multiple injections to a single brain template for each species (Majka et al. 2016). This analysis confirms that, despite the similarity in the pattern of connections, projection neurons in the marmoset

occupy a larger fraction of the cortical surface. Particularly, noticeable is the ventral extension of the main temporal lobe zone containing labeled neurons, which in marmosets invades the inferior temporal visual association cortex (cytoarchitectural area TE), although there is also greater involvement of subdivisions of area 8, and scattered labeled neurons in several other areas not evident in *Cebus*. These differences between *Cebus* and marmosets contrast with the marked similarity between *Cebus* and macaques, discussed above. Previous studies have commented on other instances of sparse projections to marmoset motor, visual and frontal areas, which had not been reported to exist in macaques (Palmer and Rosa 2006b; Reser et al. 2013; Burman et al. 2014a, 2014b).

### Connectivity as a Function of Brain Mass

The brain of *Callithrix jacchus* is 12 times smaller than that of *Macaca mulatta*, and 10 times smaller than that of *Cebus apella* (Stephan et al. 1981). This overall difference in the number of neurons may be a key factor in determining the different layouts of the network of cortico-cortical connections. It has been argued that epigenetic processes acting on different numbers of neurons may lead to different connectivity patterns, despite fundamentally similar architectures (Striedter 2005). In particular, a model has been proposed whereby, as the brain is scaled down in size, there needs to be a corresponding increase in the percent connectivity (i.e., the fraction of cells with which any one cell communicates directly) due to factors that include the metabolic cost of axonal projections, developmental constraints related to the need to increase the volume of white matter, and the availability of synaptic space on the membrane of individual neurons (Ringo 1991). As a consequence, overall brain size is expected to correlate with the level of anatomical integration across the nodes of a network, with smaller species likely to show wider anatomical integration (see also Changizi and Shimojo 2005).

The above prediction aligns well with the observed similarity between *Cebus* and macaques, despite the greater evolutionary (genetic) distance between these species (Fig. 14), and the wider network of area 10 connections observed in the marmoset. Further support for a relationship between brain mass and percent connectivity can benefit from quantitative studies in a wider range of primate species, although, crucially, there are

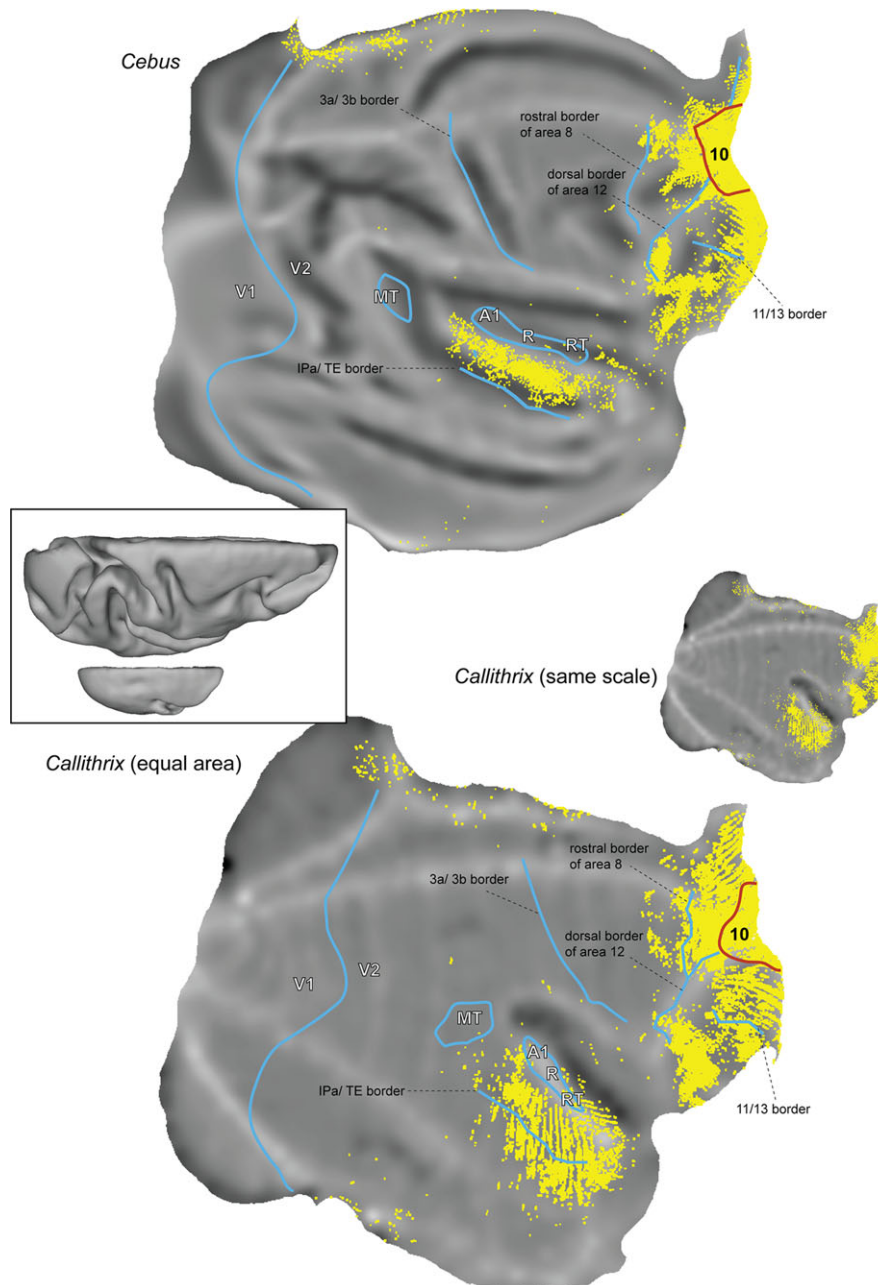


**Figure 15.** Comparison between the full patterns of cortical afferents to area 10 in *Cebus* and marmoset monkeys. These summary “unfolded” views were prepared using the coregistration method described by Majka et al. (2016), which brings results from different animals to the same stereotaxic space. Marmoset data obtained from the Marmoset Brain Architecture Project (<http://marmoset.braincircuits.org>). *Top*: Seven injections restricted to area 10, from the present sample. Each yellow point represents a labeled neuron. *Bottom*: Four injections originally reported by Burman et al. (2011b), reanalyzed for the present study. The marmoset cortex is represented in actual scale, relative to that of the *Cebus* (center right), and then reproduced with equal area (bottom). For orientation, the borders of area 10 (red) and several other histological borders that are distinctive in both species (blue) are shown. 3a and 3b, border between the subdivisions of the primary somatosensory cortex; A1/R/RT, primary, rostral, and rostrottemporal auditory core fields; MT, middle temporal area; V1 and V2, primary and second visual areas. *Insert*: Dorsal views of computer reconstructions of the *Cebus* (top) and *Callithrix* (bottom) brains, shown at the same scale.

no living marmoset-sized Old World monkeys (the smallest species being the Angolan talapoin, with a body weight of ~1.4 kg). Extrapolation of the pattern observed across monkeys with different brain sizes supports the expectation that the human brain will exhibit an even higher specificity of anatomical connections between cortical areas, potentially leading to greater susceptibility to functional loss due to the interruption of connection pathways (Horvat et al. 2016).

Earlier comparative work has highlighted the fact that brain mass (and hence number of neurons) is a factor which can account for a large percentage of the variance in the relative size of individual areas in the primate cortex (Chaplin et al. 2013). Nonetheless, it has also been acknowledged that some of the variation in the relationships between the size and location of specific structures and brain volume could be attributable to other factors, including postnatal plasticity that is mediated by

environmental interactions, and natural selection towards preservation of specific populations of neurons according to ecological niche (e.g., Kaskan et al., 2005). Is it likely, therefore, that factors other than brain size could have contributed to the present observations? The essential similarity between capuchins and macaques suggests that behavioral differences between these species (which are significant) have not impacted on the network of frontal pole connections. Nonetheless it is possible, at least in principle, that the connective differences observed between marmosets and the other species considered in the present study are determined by factors (genetic or epigenetic) related to ecological niche. However, marmosets, like capuchins, are largely arboreal primates, and, together with both macaques and capuchins, they have diurnal habits (Solomon and Rosa 2014), and live in large family groups characterized by complex social interactions (Miller et al. 2016). The most distinctive attributes of marmosets, which could be expected to have an impact on cortical organization, are the lack of dexterous hands, the presence of claws and other adaptations to vertically cling to trees, locomotion largely based on leaping, and biparental care of their young (Wahad et al. 2015). It would be difficult to pinpoint an aspect of the marmoset ecological niche that reasonably correlates with the present observations about the frontal pole cortex, given current theories about the function of this part of the primate brain (Mansouri et al. 2017).

Another possibility is that the wider connectivity of the marmoset frontal pole is related to allometry. It has been proposed that the selective expansion of brain structures could lead to wider connectivity (the “large means well connected” principle; Striedter 2005). However, we believe that the relationship we observed is the opposite of what would be expected: the frontal pole cortex expands selectively relative to other cortical areas as a function of brain size, being relatively larger in the macaque and capuchin (Chaplin et al. 2013). Thus, if anything, one would expect that the frontal pole would form more widespread connectivity in these species.

### Possible Limitations of the Present Study

One possible limitation of our analyses, which needs to be kept in mind, is the fact that the areas of association cortex in *Cebus* have not been extensively explored with physiological techniques. Thus, attempts to discuss function are necessarily based on comparisons with other species, including the macaque monkey in particular, and attempts at establishing homologies are based primarily on histology and location relative to sulci. However, we do not consider this a serious limitation. Although the information about the superior temporal cortex in *Cebus* is presently limited to behavioral lesion studies (e.g., Colombo et al. 1996), work in other systems of cortical areas has highlighted the essential similarity of function between corresponding parts of the brain in *Cebus* and *Macaca* (e.g., Felleman et al. 1983; Flament and Hore 1988; Fiorani et al. 1989; Rosa et al. 1993; Tian and Lynch 1995, 1996; Leichnetz 2001; Middleton and Strick 2002; Dum and Strick 2005; Lima et al. 2005; Padberg et al. 2007; Côté et al. 2017). When judged in light of the fact that the cytoarchitectural criteria established for the macaque were found to apply well to the *Cebus* frontal and temporal areas (Cruz-Rizzolo et al. 2011; present observations) and the essentially identical patterns of connections of the frontal pole revealed for the 2 species (see above), the most parsimonious interpretation of the available data is that the information gathered in the macaque is likely to be a valid guide to the functions of the homologous areas in *Cebus*.

A second limitation is the fact that our analysis was conducted by sampling one in 10 sections (that is, 50  $\mu$ m sections every 500  $\mu$ m). Although this means that the absolute numbers of neurons projecting to each injection site were underestimated, the proportions of cells in the different cytoarchitectural areas were most likely not seriously affected, given the relatively modest variation in cell body size in isocortical association areas (Elston and Rosa 1997, 1998). However, it is possible that very sparse connections were not detected, for any given injection.

A final limitation comes from the basic fact that areas were identified based on cytoarchitectural criteria. Many of the cytoarchitectural borders in association cortex are subtle (Rosa and Tweedale 2005; Burman et al. 2006), and there is some room for imprecision, which may have affected the exact assignment of labeled neurons to one of 2 adjacent areas. Nonetheless, we believe that our main findings are robust, being based on comparisons involving larger regions of cortex, each containing several cytoarchitectural areas (e.g., orbitofrontal cortex, dorsolateral prefrontal cortex, auditory cortex, superior temporal cortex, retrosplenial cortex).

### Conclusions

In summary, the present study provides conclusive evidence that area 10 in nonhuman primates is not uniform, in particular with respect to the fact that its lateral sector is primarily connected to other frontal association areas, whereas the medial sector receives more substantial projections from sensory (primarily auditory association and polysensory temporal) areas. Other gradients of connections, for example with respect to emphasis on projections from orbitofrontal versus dorsolateral prefrontal areas, are also suggested by our data, but require a more extensive study if they are to be mapped with precision. In addition, we propose that the most parsimonious interpretation of the present data reflects the idea that there is an essential similarity in the way that the primate cerebral cortex is organized (Chaplin et al. 2013; Gabi et al. 2016; Herculano-Houzel et al. 2016), with differences in the patterns of connections being determined to a large extent by brain mass (and, consequently, number of neurons). However, the developmental mechanism underlying such differences remains to be determined.

### Funding

This work was funded by grants from the Australian Research Council (DE120102883, DP140101968, and CE140100007); National Health and Medical Research Council (1020839 and 1082144); European Research Council (FP7-PEOPLE-2011-IOF 300452); Conselho Nacional de Pesquisa (CNPq); and Fundação Carlos Chagas Filho de Amparo à Pesquisa do Estado do Rio de Janeiro (FAPERJ).

### Notes

The authors thank Rowan Tweedale for comments on the final versions of this manuscript. *Conflict of Interest*: None declared.

### References

- Barbas H. 1988. Anatomic organization of basoventral and medio-dorsal visual recipient prefrontal regions in the rhesus monkey. *J Comp Neurol*. 276:313–342.
- Barbas H, Ghashghaei H, Dombrowski SM, Rempel-Clower NL. 1999. Medial prefrontal cortices are unified by common connections with superior temporal cortices and distinguished

- by input from memory-related areas in the rhesus monkey. *J Comp Neurol.* 410:343–367.
- Baylis GC, Rolls ET, Leonard CM. 1987. Functional subdivisions of the temporal lobe neocortex. *J Neurosci.* 7:330–342.
- Blatt GJ, Pandya DN, Rosene DL. 2003. Parcellation of cortical afferents to three distinct sectors in the parahippocampal gyrus of the rhesus monkey: an anatomical and neurophysiological study. *J Comp Neurol.* 466:161–179.
- Bludau S, Eickhoff SB, Mohlberg H, Caspers S, Laird AR, Fox PT, Schleicher A, Zilles K, Amunts K. 2014. Cytoarchitecture, probability maps and functions of the human frontal pole. *NeuroImage.* 93:260–275.
- Bortoff GA, Strick PL. 1993. Corticospinal terminations in two new-world primates: further evidence that corticomotoneuronal connections provide part of the neural substrate for manual dexterity. *J Neurosci.* 13:5105–5118.
- Burgess PW, Gilbert SJ, Dumontheil I. 2007. Function and localization within rostral prefrontal cortex (area 10). *Philos Trans R Soc Lond B Biol Sci.* 362:887–899.
- Burman KJ, Bakola S, Richardson KE, Reser DH, Rosa MGP. 2014a. Patterns of cortical input to the primary motor area in the marmoset monkey. *J Comp Neurol.* 522:811–843.
- Burman KJ, Bakola S, Richardson KE, Reser DH, Rosa MGP. 2014b. Patterns of afferent input to the caudal and rostral areas of the dorsal premotor cortex (6DC and 6DR) in the marmoset monkey. *J Comp Neurol.* 522:3683–3716.
- Burman KJ, Bakola S, Richardson KE, Yu HH, Reser DH, Rosa MGP. 2015. Cortical and thalamic projections to cytoarchitectural areas 6Va and 8C of the marmoset monkey: connectionally distinct subdivisions of the lateral premotor cortex. *J Comp Neurol.* 523:1222–1247.
- Burman KJ, Palmer SM, Gamberini M, Rosa MGP. 2006. Cytoarchitectonic subdivisions of the dorsolateral frontal cortex of the marmoset monkey (*Callithrix jacchus*), and their projections to dorsal visual areas. *J Comp Neurol.* 495:149–172.
- Burman KJ, Reser DH, Richardson KE, Gaulke H, Worthy KH, Rosa MGP. 2011a. Subcortical projections to the frontal pole in the marmoset monkey. *Eur J Neurosci.* 34:303–319.
- Burman KJ, Reser DH, Yu H-H, Rosa MGP. 2011b. Cortical input to the frontal pole of the marmoset monkey. *Cereb Cortex.* 21:1712–1737.
- Carmichael ST, Price JL. 1995. Sensory and premotor connections of the orbital and medial prefrontal cortex of macaque monkeys. *J Comp Neurol.* 363:642–664.
- Cavada C, Company T, Tejedor J, Cruz-Rizzolo RJ, Reinoso-Suarez F. 2000. The anatomical connections of the macaque monkey orbitofrontal cortex. A review. *Cereb Cortex.* 10:220–242.
- Changizi MA, Shimojo S. 2005. Parcellation and area-area connectivity as a function of neocortex size. *Brain Behav Evol.* 66:88–98.
- Chaplin TA, Yu HH, Soares JG, Gattass R, Rosa MGP. 2013. A conserved pattern of differential expansion of cortical areas in simian primates. *J Neurosci.* 33:15120–15125.
- Chatterjee HJ, Ho SY, Barnes I, Groves C. 2009. Estimating the phylogeny and divergence times of primates using a supermatrix approach. *BMC Evol Biol.* 9:259.
- Colombo M, Rodman HR, Gross CG. 1996. The effects of superior temporal cortex lesions on the processing and retention of auditory information in monkeys (*Cebus apella*). *J Neurosci.* 16:4501–4517.
- Condé F. 1987. Further studies on the use of the fluorescent tracers fast blue and diamidino yellow: effective uptake area and cellular storage sites. *J Neurosci Methods.* 21:31–43.
- Côté SL, Hamadjida A, Quessy S, Dancause N. 2017. Contrasting modulatory effects from the dorsal and ventral premotor cortex on primary motor cortex outputs. *J Neurosci.* 37:5960–5973.
- Cruz-Rizzolo RJ, De Lima MA, Ervolino E, de Oliveira JA, Casatti CA. 2011. Cyto-, myelo- and chemoarchitecture of the prefrontal cortex of the Cebus monkey. *BMC Neurosci.* 12:1–26.
- Dum RP, Strick PL. 2005. Frontal lobe inputs to the digit representations of the motor areas on the lateral surface of the hemisphere. *J Neurosci.* 25:1375–1386.
- Elston GN, Rosa MGP. 1997. The occipitoparietal pathway of the macaque monkey: comparison of pyramidal cell morphology in layer III of functionally related cortical visual areas. *Cereb Cortex.* 7:432–452.
- Elston GN, Rosa MGP. 1998. Morphological variation of layer III pyramidal neurones in the occipitotemporal pathway of the macaque monkey visual cortex. *Cereb Cortex.* 8:278–294.
- Felleman DJ, Nelson RJ, Sur M, Kaas JH. 1983. Representations of the body surface in areas 3b and 1 of postcentral parietal cortex of *Cebus* monkeys. *Brain Res.* 268:15–26.
- Fiorani M Jr, Gattass R, Rosa MGP, Sousa AP. 1989. Visual area MT in the *Cebus* monkey: location, visuotopic organization, and variability. *J Comp Neurol.* 287:98–118.
- Flament D, Hore J. 1988. Relations of motor cortex neural discharge to kinematics of passive and active elbow movements in the monkey. *J Neurophysiol.* 60:1268–1284.
- Gabi M, Neves K, Masseron C, Ribeiro PF, Ventura-Antunes L, Torres L, Mota B, Kaas JH, Herculano-Houzel S. 2016. No relative expansion of the number of prefrontal neurons in primate and human evolution. *Proc Natl Acad Sci USA.* 113:9617–9622.
- Galaburda AM, Pandya DN. 1983. The intrinsic architectonic and connective organization of the superior temporal region of the rhesus monkey. *J Comp Neurol.* 221:169–184.
- Gallyas F. 1979. Silver staining of myelin by means of physical development. *Neurol Res.* 1:203–209.
- Hackett TA, Stepniewska I, Kaas JH. 1999. Prefrontal connections of the parabelt auditory cortex in macaque monkeys. *Brain Res.* 817:45–58.
- Herculano-Houzel S, Kaas JH, de Oliveira-Souza R. 2016. Corticalization of motor control in humans is a consequence of brain scaling in primate evolution. *J Comp Neurol.* 524:448–455.
- Horvat S, Gamanut R, Ercsey-Ravasz M, Magrou L, Gamanut B, Van Essen DC, Burkhalter A, Knoblauch K, Toroczkai Z, Kennedy H. 2016. Spatial embedding and wiring cost constrain the functional layout of the cortical network of rodents and primates. *PLoS Biol.* 14:e1002512.
- Jacobson S, Trojanowski JQ. 1977. Prefrontal granular cortex of the rhesus monkey. I. Intrahemispheric cortical afferents. *Brain Res.* 132:209–233.
- Kajikawa Y, Frey S, Ross D, Falchier A, Hackett TA, Schroeder CE. 2015. Auditory properties in the parabelt regions of the superior temporal gyrus in the awake macaque monkey: an initial survey. *J Neurosci.* 35:4140–4150.
- Kaskan PM, Franco EC, Yamada ES, Silveira LC, Darlington RB, Finlay BL. 2005. Peripheral variability and central constancy in mammalian visual system evolution. *Proc R Soc B.* 272:91–100.
- Kobayashi Y, Amaral DG. 2000. Macaque monkey retrosplenial cortex: I. three-dimensional and cytoarchitectonic organization. *J Comp Neurol.* 426:339–365.
- Koechlin E. 2011. Frontal pole function: what is specifically human? *Trends Cogn Sci.* 15:241.
- Krubitzer L. 2009. In search of a unifying theory of complex brain evolution. *Ann NY Acad Sci.* 1156:44–67.

- Le Gros Clark WE. 1959. *The Antecedents of Man*. Edinburgh: Edinburgh University Press.
- Leichnetz GR. 2001. Connections of the medial posterior parietal cortex (area 7m) in the monkey. *Anat Rec*. 263:215–236.
- Lima B, Fiorani M, Gattass R. 2005. Changes of ongoing activity in *Cebus* monkey perirhinal cortex correlate with behavioral performance. *Braz J Med Biol Res*. 38:59–63.
- Liu H, Qin W, Li W, Fan L, Wang J, Jiang T, Yu C. 2013. Connectivity-based parcellation of the human frontal pole with diffusion tensor imaging. *J Neurosci*. 33:6782–6790.
- Majka P, Chaplin TA, Yu H-H, Tolpygo A, Mitra PP, Wojcik DK, Rosa MGP. 2016. Towards a comprehensive atlas of cortical connections in a primate brain: mapping tracer injection studies of the common marmoset into a reference digital template. *J Comp Neurol*. 524:2161–2181.
- Mansouri FA, Koehlin E, Rosa MGP, Buckley MJ. 2017. Managing competing goals—a key role for the frontopolar cortex. *Nat Rev Neurosci*. 18:645–657.
- Mansouri FA, Rosa MGP, Atapour N. 2015. Working memory in the service of executive control functions. *Front Syst Neurosci*. 9:166.
- Mayer A, Nascimento-Silva ML, Keher NB, Bittencourt-Navarrete RE, Gattass R, Franca JG. 2016. Architectonic mapping of somatosensory areas involved in skilled forelimb movements and tool use. *J Comp Neurol*. 524:1399–1423.
- Medalla M, Barbas H. 2014. Specialized prefrontal “auditory fields”: organization of primate prefrontal-temporal pathways. *Front Neurosci*. 8:77.
- Middleton FA, Strick PL. 2002. Basal-ganglia ‘projections’ to the prefrontal cortex of the primate. *Cereb Cortex*. 12:926–935.
- Mikellidou K, Kurzawski JW, Frijia F, Montanaro D, Greco V, Burr DC, Morrone MC. 2017. Area prostriata in the human brain. *Curr Biol*. 27:3056–3060.
- Miller CT, Freiwald WA, Leopold DA, Mitchell JF, Silva AC, Wang X. 2016. Marmosets: a neuroscientific model of human social behavior. *Neuron*. 90:219–233.
- Moayed M, Salomons TV, Dunlop KA, Downar J, Davis KD. 2015. Connectivity-based parcellation of the human frontal polar cortex. *Brain Struct Funct*. 220:2603–2616.
- Morecraft RJ, Rockland KS, Van Hoesen GW. 2000. Localization of area prostriata and its projection to the cingulate motor cortex in the rhesus monkey. *Cereb Cortex*. 10:192–203.
- Munoz-Lopez MM, Mohedano-Moriano A, Insausti R. 2010. Anatomical pathways for auditory memory in primates. *Front Neuroanat*. 4:129.
- Neubert FX, Mars RB, Thomas AG, Sallet J, Rushworth MF. 2014. Comparison of human ventral frontal cortex areas for cognitive control and language with areas in monkey frontal cortex. *Neuron*. 81:700–713.
- Öngür D, Ferry AT, Price JL. 2003. Architectonic subdivision of the human orbital and medial prefrontal cortex. *J Comp Neurol*. 460:425–449.
- Orr JM, Smolker HR, Banich MT. 2015. Organization of the human frontal pole revealed by large-scale dti-based connectivity: implications for control of behavior. *PLoS One*. 10:e0124797.
- Padberg J, Franca JG, Cooke DF, Soares JG, Rosa MGP, Fiorani MJ, Gattass R, Krubitzer L. 2007. Parallel evolution of cortical areas involved in skilled hand use. *J Neurosci*. 27:10106–10115.
- Palmer SM, Rosa MGP. 2006a. A distinct anatomical network of cortical areas for analysis of motion in far peripheral vision. *Eur J Neurosci*. 24:2389–2405.
- Palmer SM, Rosa MGP. 2006b. Quantitative analysis of the corticocortical projections to the middle temporal area in the marmoset monkey: evolutionary and functional implications. *Cereb Cortex*. 16:1361–1375.
- Passarelli L, Rosa MGP, Bakola S, Gamberini M, Worthy KH, Fattori P, Galletti C. 2017. Uniformity and diversity of cortical projections to precuneate areas in the macaque monkey: what defines area PGM? *Cereb Cortex*. doi:10.1093/cercor/bhx067[Epub ahead of print].
- Paxinos G, Watson C, Petrides M, Rosa M, Tokuno H. 2012. *The marmoset brain in stereotaxic coordinates*. London: Academic Press, Elsevier, Inc.
- Perelman P, Johnson WE, Roos C, Seuanez HN, Horvath JE, Moreira MA, Kessing B, Pontius J, Roelke M, Rumpel Y, et al. 2011. A molecular phylogeny of living primates. *PLoS Genet*. 7:e1001342.
- Perez SI, Klaczko J, dos Reis SF. 2012. Species tree estimation for a deep phylogenetic divergence in the New World monkeys (Primates: *Platyrrhini*). *Mol Phylogenet Evol*. 65:621–630.
- Petrides M, Pandya DN. 1999. Dorsolateral prefrontal cortex: comparative cytoarchitectonic analysis in the human and the macaque brain and corticocortical connection patterns. *Eur J Neurosci*. 11:1011–1036.
- Petrides M, Pandya DN. 2007. Efferent association pathways from the rostral prefrontal cortex in the macaque monkey. *J Neurosci*. 27:11573–11586.
- Phillips K, Sherwood C, Lilak A. 2007. Corpus callosum morphology in capuchin monkeys is influenced by sex and handedness. *PLoS One*. 2:e792.
- Ramnani N, Owen AM. 2004. Anterior prefrontal cortex: insights into function from anatomy and neuroimaging. *Nat Rev Neurosci*. 5:184–194.
- Ray KL, Zald DH, Bludau S, Riedel MC, Bzdok D, Yanes J, Falcone KE, Amunts K, Fox PT, Eickhoff SB, et al. 2015. Co-activation based parcellation of the human frontal pole. *NeuroImage*. 123:200–211.
- Reser DH, Burman KJ, Richardson KE, Spitzer MW, Rosa MGP. 2009. Connections of the marmoset rostrotemporal auditory area: express pathways for analysis of affective content in hearing. *Eur J Neurosci*. 30:578–592.
- Reser DH, Burman KJ, Yu HH, Chaplin TA, Richardson KE, Worthy KH, Rosa MGP. 2013. Contrasting patterns of cortical input to architectural subdivisions of the area 8 complex: a retrograde tracing study in marmoset monkeys. *Cereb Cortex*. 23:1901–1922.
- Reser DH, Richardson KE, Montibeller MO, Zhao S, Chan JM, Soares JG, Chaplin TA, Gattass R, Rosa MGP. 2014. Claustrum projections to prefrontal cortex in the capuchin monkey (*Cebus apella*). *Front Syst Neurosci*. 8:123.
- Ringo JL. 1991. Neuronal interconnection as a function of brain size. *Brain Behav Evol*. 38:1–6.
- Rosa MGP, Soares JG, Fiorani MJ, Gattass R. 1993. Cortical afferents of visual area MT in the *Cebus* monkey: possible homologies between New and Old World monkeys. *Vis Neurosci*. 10:827–855.
- Rosa MGP, Tweedale R. 2005. Brain maps, great and small: lessons from comparative studies of primate visual cortical organization. *Philos Trans R Soc Lond B Biol Sci*. 360:665–691.
- Saleem KS, Kondo H, Price JL. 2008. Complementary circuits connecting the orbital and medial prefrontal networks with the temporal, insular, and opercular cortex in the macaque monkey. *J Comp Neurol*. 506:659–693.
- Saleem KS, Miller B, Price JL. 2014. Subdivisions and connective networks of the lateral prefrontal cortex in the macaque monkey. *J Comp Neurol*. 522:1641–1690.
- Schmued LC. 1990. A rapid, sensitive histochemical stain for myelin in frozen brain sections. *J Histochem Cytochem*. 38:717–720.

- Seltzer B, Pandya DN. 1978. Afferent cortical connections and architectonics of the superior temporal sulcus and surrounding cortex in the rhesus monkey. *Brain Res.* 149:1–24.
- Semendeferi K, Armstrong E, Schleicher A, Zilles K, Van Hoesen GW. 2001. Prefrontal cortex in humans and apes: a comparative study of area 10. *Am J Phys Anthropol.* 114:224–241.
- Solomon SG, Rosa MGP. 2014. A simpler primate brain: the visual system of the marmoset monkey. *Front Neural Circuits.* 8:96.
- Steiper ME, Young NM. 2006. Primate molecular divergence dates. *Mol Phylogenet Evol.* 41:384–394.
- Stephan H, Frahm H, Baron G. 1981. New and revised data on volumes of brain structures in insectivores and primates. *Folia Primatol (Basel).* 35:1–29.
- Striedter GF. 2005. *Principles of brain evolution.* Sunderland, MA: Sinauer.
- Tian JR, Lynch JC. 1995. Slow and saccadic eye movements evoked by microstimulation in the supplementary eye field of the *Cebus* monkey. *J Neurophysiol.* 74:2204–2210.
- Tian JR, Lynch JC. 1996. Functionally defined smooth and saccadic eye movement subregions in the frontal eye field of *Cebus* monkeys. *J Neurophysiol.* 76:2740–2753.
- Tranel D, Brady DR, Van Hoesen GW, Damasio AR. 1988. Parahippocampal projections to posterior auditory association cortex (area Tpt) in Old-World monkeys. *Exp Brain Res.* 70:406–416.
- Tsujimoto S, Genovesio A, Wise SP. 2011. Frontal pole cortex: encoding ends at the end of the endbrain. *Trends Cogn Sci.* 15:169–176.
- Van Essen DC, Drury HA, Dickson J, Harwell J, Hanlon D, Anderson CH. 2001. An integrated software suite for surface-based analyses of cerebral cortex. *J Am Med Inform Assoc.* 8:443–459.
- Wahad F, Drummer C, Behr R. 2015. Marmosets. *Curr Biol.* 25:R775–R792.
- Wong-Riley M. 1979. Changes in the visual system of monocularly sutured or enucleated cats demonstrable with cytochrome oxidase histochemistry. *Brain Res.* 171:11–28.
- Yu HH, Chaplin TA, Davies AJ, Verma R, Rosa MGP. 2012. A specialized area in limbic cortex for fast analysis of peripheral vision. *Curr Biol.* 22:1351–1357.